Chemical Thermodynamics and Thermal Analysis 20 (2025) 100214

Contents lists available at ScienceDirect

Chemical Thermodynamics and Thermal Analysis

journal homepage: www.elsevier.com/locate/ctta

# Thermophysical and spectroscopic study of molecular interactions in 1-butyl-3-methylimidazolium tetrafluoroborate + propyl acetate system at ambient temperatures: Experimental and theoretical approach

M. Durga Bhavani [a], T.S. Krishna [b,*], A. Hernandez [c], A.K. Nain [d,*]

[a] Department of Chemistry, V. R. Siddhartha Engineering College, Kanuru, Vijayawada 520007, India
[b] Department of Physics, P. B. Siddhartha College of Arts & Science, Vijayawada 520010, India
[c] Facultad de Ingeniería y Negocios, Universidad de Las Américas, Concepción 4030000, Chile
[d] Department of Chemistry, Dyal Singh College, University of Delhi, New Delhi 110003, India

ARTICLE INFO

*Keywords:*
[BMIM][$BF_4$]
propyl acetate, molecular interactions
PC-SAFT model
PFP theory

ABSTRACT

The study presents the investigation of molecular interactions in blended mixtures of 1-butyl-3-methylimidazolium tetrafluoroborate [BMIM][$BF_4$] + propyl acetate from the measurements of density, $\rho$ and speed of sound, $u$ of pure 1-butyl-3-methylimidazolium tetrafluoroborate [BMIM][$BF_4$], propyl acetate and their mixtures across entire mole fraction range at temperature from 298.15 – 323.15 K with an interval of 5 K and at pressure, $p = 100$ kPa. The excess properties for the mixtures, partial molar properties (volume/compressibility), excess partial molar properties (volume/compressibility) of the components across entire mole fraction range; and at infinite dilution were been calculated. The excess molar volumes of these mixtures were predicted theoretically using PFP theory and the results were compared with experimental values. The density data of these mixtures was modelled using PC-SAFT model, whereas a number of models were applied to predict the speed of sound theoretically. Additionally, the FT-IR spectra of pure [BMIM][$BF_4$], propyl acetate and their near equimolar mixture were recorded and examined to validate the nature and extent of dominant intermolecular interactions.

## 1. Introduction

The study of molecular interactions by means of volumetric and acoustic properties provides valuable insight into the behaviour of ionic liquids in different solvent systems. This research focuses on 1-butyl-3-methyl Imidazolium tetrafluoroborate [BMIM][$BF_4$] a commonly used ionic liquid and its interactions with propyl acetate, an organic ester. Ionic liquids, like [BMIM][$BF_4$] have gained attention owing to their exceptional physicochemical properties, such as low volatility, high thermal stability and tuneable solvation capabilities, which make them ideal candidates for various applications in green chemistry, catalysis, and separation processes [1–13].

Volumetric and acoustic studies, such as density, speed of sound and derived excess parameters are essential for understanding the molecular interactions between solutes and solvents. These properties help decipher the nature of interactions like hydrogen bonding, van der Waals forces, and dipole interactions between [BMIM][$BF_4$] and propyl acetate. Investigating how these interactions influence structural arrangement and solvent behaviour at the molecular level provides crucial information for optimizing the usage of ionic liquids in industrial processes. This work aims to explore the thermodynamic properties of [BMIM][$BF_4$] + propyl acetate mixtures across entire concentration range at different temperatures, offering a comprehensive view of the interaction mechanism involved. By analysing the volumetric and acoustic parameters, this study contributes to the understanding of ionic liquid-solvent systems, potentially enhancing the design and application of ionic liquids in various technological fields.

This study presents the densities, $\rho$ and speeds of sound, $u$ for the blended mixtures of [BMIM][$BF_4$] with propyl acetate, covering the complete range of mole fractions at the temperatures, $T = (298.15 – 323.15)$ K at 5 K increments at pressure, $p = 100$ kPa. Excess properties, partial molar properties (volume/compressibility), and excess partial molar properties (volume/compressibility) of the components have been determined across the complete mole fraction range and at infinite dilution. The parameters of these factors concerning composition and temperature are discussed in terms of intermolecular interactions within

* Corresponding authors.
*E-mail addresses:* sritadikonda@gmail.com (T.S. Krishna), anilkumarnain@dsc.du.ac.in (A.K. Nain).

https://doi.org/10.1016/j.ctta.2025.100214
Received 3 July 2025; Received in revised form 12 August 2025; Accepted 25 August 2025
Available online 27 August 2025

these mixtures. The experimental values of $\rho$ and $u$ were correlated using the Jouyban-Acree model [14,15] in order to establish their dependence on composition and temperature. The perturbed chain statistical associating fluid theory (PC-SAFT) equation of state (EoS) [16,17] was used to calculate the compressed liquid density for these mixtures at various molar compositions and temperatures. The $u$ values of these mixtures were theoretically computed from various theories and relations and the outcomes are equated to the experimental data.

## 2. Experimental

### 2.1. Materials

The IL [BMIM][$BF_4$], with a mass fraction purity of 0.995, was obtained from Iolitec GmbH in Germany, whereas propyl acetate, with a mass fraction purity of 0.98, was sourced from Sigma-Aldrich in India. The specifics regarding the chemicals employed are presented in Table 1. Prior to the preparation of the solutions, all chemicals underwent a degassing process utilising an ultrasonic cleaner. All chemical purity and water content were assessed by GC [18] and Karl Fisher titration method (Metrohm, 890 Titrando) [19]. The sample preparation was given in our previous paper [20].

### 2.2. Measurements

The sample's densities and speeds of sound were assessed utilising a Density and Speed of Sound Analyser (DSA 5000 M, Anton Paar, Austria) at an operational frequency of 3 MHz for $u$ measurements. The densimeter was calibrated utilising the $\rho$ and $u$ of triple-distilled water and dry air. To ascertain the density of high-viscosity liquids, the instrument was calibrated using two viscous sugar solutions to mitigate the viscosity corrections required. The temperature of the samples was regulated by an integrated Peltier device with an accuracy of ±0.01 K. The estimations of uncertainties in the measurements of $\rho$, $u$ and temperature were determined to be within ±0.8 kg·m$^{-3}$, ±0.8 m·s$^{-1}$ and ±0.01 K, respectively. The $\rho$ and $u$ values of pure ionic liquid and propyl acetate were taken from our previous studies [20,21].

## 3. Results and discussion

The measured values of $\rho$ and $u$ for [BMIM][$BF_4$] + propyl acetate mixtures all mole fractions of [BMIM][$BF_4$] and at each temperature are listed in Table 2.

### 3.1. Excess properties

The values of $V_m^E$, $\kappa_s^E$, $K_{s,m}^E$, $u^E$ and $\alpha_p^E$ were calculated from the measured values of $\rho$ and $u$ by the using standard relations reported in the literature [22–24]. The values of $V_m^E$ has been calculated using the following relation

$$V_m^E = V_m - V_m^{id} = \frac{x_1M_1 + x_2M_2}{\rho} - \left(\frac{x_1M_1}{\rho_1} + \frac{x_2M_2}{\rho_2}\right) \quad (1)$$

where $x$ is mole fraction, $M$ is molar masses, and the subscripts 1 and 2 refer to the pure liquid components, [BMIM][$BF_4$] and propyl acetate, respectively; superscript 'id' represents value for ideal mixture.

The isentropic compressibility, $\kappa_s$ has been calculated from the measured density and speed of sound values using the Newton-Laplace equation

$$\kappa_s = -V_m^{-1}(\partial V_m/\partial P)_s = (\rho u^2)^{-1} \quad (2)$$

Molar isentropic compressibility, $K_{s,m}$ has been calculated by the relation

$$K_{s,m} = -(\partial V/\partial P)_S = \kappa_s V \quad (3)$$

The values of $\kappa_s^E$, $K_{s,m}^E$, $u^E$ and $\alpha_p^E$ [25] were calculated by using the following equations

$$\kappa_s^E = \kappa_s - \kappa_s^{id} \quad (4)$$

$$K_{s,m}^E = K_{s,m} - K_{s,m}^{id} \quad (5)$$

$$u^E = u - \left(\rho^{id}\kappa_s^{id}\right)^{-1/2} \quad (6)$$

$$\alpha_p^E = \alpha_p - \alpha_p^{id} \quad (7)$$

The values of $\kappa_s^{id}$ and $K_{s,m}^{id}$ values for binary mixtures are calculated by means of relations [24]

$$k_s^{id} = \phi_1 k_{s,1} + \phi_2 k_{s,2} + T\left[\frac{\phi_1 V_{m,1}(\alpha_{p,1})^2}{C_{p,1}} + \frac{\phi_2 V_{m,2}(\alpha_{p,2})^2}{C_{p,2}} + \frac{V_m^{id}\left(\alpha_p^{id}\right)^2}{C_p^{id}}\right] \quad (8)$$

$$K_{s,m}^{id} = x_1 K_{s,m,1} + x_2 K_{s,m,2} + T\left[\frac{x_1 V_{m,1}(\alpha_{p,1})^2}{C_{p,1}} + \frac{x_2 V_{m,2}(\alpha_{p,2})^2}{C_{p,2}} + \frac{V_m^{id}\left(\alpha_p^{id}\right)^2}{C_p^{id}}\right] \quad (9)$$

where $\phi$, $\alpha_p$, and $C_p$ are the volume fraction, isobaric expansivity and molar isobaric heat capacity, respectively. The values of $\phi$, $\alpha_p$, $V_m^{id}$, $\alpha_p^{id}$ and $C_p^{id}$ are calculated using the following relations [22–24]

$$\phi_i = x_i V_{m,i} \Big/ \left(\sum_{i=1}^{2} x_i V_{m,i}\right) \quad (10)$$

$$\alpha_p = -\frac{1}{\rho}\left(\frac{\partial \rho}{\partial T}\right)_p \quad (11)$$

$$V_m^{id} = x_1 V_{m,1} + x_2 V_{m,2} \quad (12)$$

$$\alpha_p^{id} = \phi_1 \alpha_{p,1} + \phi_2 \alpha_{p,2} \quad (13)$$

$$C_p^{id} = x_1 C_{p,1} + x_2 C_{p,2} \quad (14)$$

The group contribution method was utilised to assess the $C_p$ values of the pure liquids [26]. The value of $V_m^E$, $\kappa_s^E$, $K_{s,m}^E$, $u^E$ and $\alpha_p^E$ at all mole fractions, $x_1$ of [BMIM][$BF_4$] and temperature for the system are recorded in Table 3.

**Table 1**
Specification of chemicals.

| Chemical name (CAS number) | Source | Initial mass fraction purity | Purification method | Final Mass fraction purity | Water content (ppm) (KF)[a] | Analysis method |
|---|---|---|---|---|---|---|
| [BMIM][$BF_4$] (174501-65-6) | Iolitech, Germany | > 0.995 | Degassed under vacuum | - | < 40 | NA |
| Propyl acetate (109-60-4) | Spectrochem, India | > 0.98 | Degassed under vacuum | > 0.993 | < 50 | GC[b] |

[a] KF = Karl-Fischer titration.
[b] GC = Gas chromatography.

**Table 2**
Densities, $\rho$/kg·m$^{-3}$ and speeds of sound, $u$/m·s$^{-1}$ at each mole fraction, $x_1$ of [BMIM][$BF_4$] for [BMIM][$BF_4$] + propyl acetate mixtures at the temperatures, $T$/K = (293.15 – 323.15) and pressure, $p$ = 100 kPa[a].

| $x_1$ | $T$/K | | | | | |
|---|---|---|---|---|---|---|
| | 298.15 | 303.15 | 308.15 | 313.15 | 318.15 | 323.15 |
| $\rho$/kg·m$^{-3}$ | | | | | | |
| 0.0000 | 882.82 [21] | 877.19 [21] | 871.55 [21] | 865.88 [21] | 860.18 [21] | 854.46 [21] |
| 0.0985 | 933.05 | 927.28 | 920.80 | 915.15 | 909.49 | 903.86 |
| 0.1999 | 978.39 | 972.67 | 966.14 | 960.62 | 955.06 | 949.53 |
| 0.2916 | 1014.77 | 1009.21 | 1003.06 | 997.68 | 992.24 | 986.83 |
| 0.3955 | 1051.43 | 1046.13 | 1040.59 | 1035.36 | 1030.13 | 1024.88 |
| 0.5022 | 1084.76 | 1079.78 | 1074.82 | 1069.83 | 1064.80 | 1059.78 |
| 0.5932 | 1110.24 | 1105.54 | 1100.96 | 1096.24 | 1091.36 | 1086.55 |
| 0.7095 | 1139.37 | 1135.00 | 1130.74 | 1126.30 | 1121.73 | 1117.24 |
| 0.7994 | 1159.60 | 1155.49 | 1151.36 | 1147.23 | 1142.86 | 1138.65 |
| 0.9023 | 1180.64 | 1176.82 | 1172.90 | 1169.07 | 1165.05 | 1161.17 |
| 1.0000 | 1198.79 [20] | 1195.18 [20] | 1191.60 [20] | 1188.04 [20] | 1184.50 [20] | 1180.98 [20] |
| $u$/m·s$^{-1}$ | | | | | | |
| 0.0000 | 1165.1 [21] | 1144.1 [21] | 1122.6 [21] | 1101.7 [21] | 1080.1 [21] | 1059.2 [21] |
| 0.0985 | 1192.7 | 1170.0 | 1146.6 | 1124.5 | 1101.8 | 1079.9 |
| 0.1999 | 1227.3 | 1203.0 | 1178.6 | 1154.3 | 1130.0 | 1106.8 |
| 0.2916 | 1262.6 | 1237.0 | 1211.4 | 1185.9 | 1160.3 | 1135.6 |
| 0.3955 | 1305.5 | 1279.0 | 1252.5 | 1226.0 | 1199.4 | 1173.6 |
| 0.5022 | 1351.6 | 1324.8 | 1297.9 | 1271.1 | 1244.3 | 1217.9 |
| 0.5932 | 1391.8 | 1365.2 | 1338.8 | 1312.4 | 1286.0 | 1260.0 |
| 0.7095 | 1442.5 | 1417.9 | 1393.3 | 1368.6 | 1344.0 | 1320.2 |
| 0.7994 | 1481.2 | 1459.1 | 1437.0 | 1414.9 | 1392.8 | 1371.8 |
| 0.9023 | 1524.6 | 1506.8 | 1489.0 | 1471.3 | 1454.5 | 1437.9 |
| 1.0000 | 1565.1 [20] | 1553.2 [20] | 1541.4 [20] | 1529.7 [20] | 1518.2 [20] | 1506.8 [20] |

[a] Standard uncertainties $s$ are $s(T) = \pm 0.01$ K, $s(x) = \pm 5.0 \times 10^{-4}$, $s(\rho) = \pm 0.8$ kg•m$^{-3}$, $s(u) = \pm 0.8$ m•s$^{-1}$, and $s(p) = \pm 5.0$ kPa.

The values of $V_m^E$, $\kappa_s^E$, $K_{s,m}^E$, $u^E$ and $\alpha_p^E$ of these mixtures have been fitted to the Redlich-Kister [27] polynomial equation

$$Y^E = x_1(1-x_1)\sum_{i=0}^{n} A_i(1-2x_1)^i \quad (15)$$

where $Y^E$ is $V_m^E$ or $\kappa_s^E$ or $K_{s,m}^E$ or $u^E$ or $\alpha_p^E$. The coefficients, $A_i$ were derived through the applications of the least squares method, treating all points with equal weight. The standard deviations of fit, $\sigma(Y^E)$, were computed using the following relation.

$$\sigma(Y^E) = \left(\frac{\sum\left(Y_{expt}^E - Y_{cal}^E\right)^2}{(m-n)}\right)^{1/2} \quad (16)$$

In this study, $m$ represents the number of experimental data points, while $n$ denotes the number of $A_i$coefficients considered, which totals $n$+1. The optimal quantity of $A_i$ coefficients were evaluated using statistical methods, specifically the F-test.

The coefficients, $A_i$ for fit of $V_m^E$, $\kappa_s^E$, $K_{s,m}^E$, $u^E$ and $\alpha_p^E$ and $\sigma(Y^E)$ are given in Table 4. The variations of $V_m^E$, $\kappa_s^E$, $K_{s,m}^E$, $u^E$ and $\alpha_p^E$ with mole fraction, $x_1$, together with the values calculated from equation (15) at each temperature, are shown graphically in Figs. 1–5, respectively.

When [BMIM][$BF_4$] is added to propyl acetate, $V_m^E$ (Fig. 1) becomes increasingly negative throughout the composition range and across all studied temperatures, indicating significant molecular interactions and structural evolution within the system. These negative deviations reflect strong specific interactions between the components, deviating from an ideal solution.

At low mole fractions of [BMIM][$BF_4$], the addition of the IL to propyl acetate leads to increasingly negative $V_m^E$ values. This is attributed to significant molecular interactions such as hydrogen bonding between $C_2$-H groups in the imidazolium ring and the carbonyl oxygen of propyl acetate [28], as well as ion-dipole interactions [29,30] and π-π stacking between the planar imidazolium ring and the aliphatic chains of the ester. These interactions lead to closer packing of molecules and reduced free volume, resulting in negative excess molar volume [31].

At intermediate mole fraction (~0.5), the magnitude of $V_m^E$ reaches a minimum, signifying the point of maximum interaction between the two components. At this composition, a well-balanced molecular network is established wherein the IL effectively disrupts the initial structure of propyl acetate and facilitates the formation of stronger and more ordered ion-molecule associations. This enhanced structuring results in the greatest reduction in $V_m^E$ and is consistent with an energetically favourable packing agreement.

At higher mole fractions [BMIM][$BF_4$], $V_m^E$ becomes less negative. This trend implies a weakening of interactions between unlike molecules as the system becomes increasingly dominated by IL-IL interactions. IL's structural ordering becomes more characteristic, and the contribution from strong ion-dipole or H-bonding with propyl acetate diminishes.

The negative values $\kappa_s^E$ observed in Fig. 3 further confirms the formation of a structurally ordered, less compressible mixture. The reduction in compressibility indicated that the interactions in the mixed system restrict molecular mobility and volume response to pressure. Supporting the idea of enhanced cohesion due to specific intermolecular forces. From an electronic perspective, the partial charge transfer or polarisation effects between the cationic imidazolium species and the ester group may involve minor orbital overlap, such as $p$-$\pi$ or $n$-$\pi^*$ interactions, which enhance structural rigidity [32]. These findings suggest that the IL + propyl acetate system exhibits significant non-ideal behaviour governed by specific ion-dipole and dispersive forces, offering a molecular-level rationale for the observed volumetric and compressibility trends.

The impact of temperature on the excess properties is also significant. As shown in Figs. 1 and 2, an increase in temperature leads to a decrease in the magnitude of both $V_m^E$ and $\kappa_s^E$ across all mole fractions. Due to enhanced molecular motion, this thermal effect can be ascribed to the disruption of specific intermolecular forces, such as H-bonding, ion-dipole, and van der Waals interactions. The weakening of these interactions with rising temperature results in a less compact structure, thereby reducing the volume contraction and rigidity of the solution [33].

As shown in Fig. 5, $K_{s,m}^E$ values are consistently negative over the entire composition range and at all studied temperatures, indicating that

**Table 3**
The values of $V_m^E$, $\kappa_s^E$, $K_{s,m}^E$, $u^E$ and $\alpha_p^E$ at each mole fraction, $x_1$ of [BMIM][$BF_4$] for [BMIM][$BF_4$] + propyl acetate mixtures at the temperatures, $T$/K = (298.15 to 323.15).

| $x_1$ | $10^6 \cdot V_m^E$/ $m^3 \bullet mol^{-1}$ | $10^{10} \cdot \kappa_s^E$/ $m^2 \bullet N^{-1}$ | $10^{14} \cdot K_{s,m}^E$/ $m^5 \bullet N^{-1} \bullet mol^{-1}$ | $10^2 \cdot u^E$/ $m \cdot s^{-1}$ | $10^4 \cdot \alpha_p^E$/ $K^{-1}$ |
|---|---|---|---|---|---|
| 298.15 K | | | | | |
| 0.0985 | -0.3229 | -0.2084 | -0.2804 | 0.1461 | -1.956 |
| 0.1999 | -0.5540 | -0.3583 | -0.5042 | 0.2862 | -3.425 |
| 0.2916 | -0.6879 | -0.4426 | -0.6485 | 0.3983 | -4.334 |
| 0.3955 | -0.7649 | -0.4851 | -0.7437 | 0.4997 | -4.924 |
| 0.5022 | -0.7688 | -0.4776 | -0.7661 | 0.5648 | -5.077 |
| 0.5932 | -0.7182 | -0.4378 | -0.7290 | 0.5821 | -4.858 |
| 0.7095 | -0.5903 | -0.3461 | -0.6043 | 0.5333 | -4.122 |
| 0.7994 | -0.4471 | -0.2536 | -0.4587 | 0.4375 | -3.200 |
| 0.9023 | -0.2359 | -0.1295 | -0.2435 | 0.2541 | -1.759 |
| 303.15 K | | | | | |
| 0.0985 | -0.2856 | -0.1930 | -0.2611 | 0.1274 | -1.896 |
| 0.1999 | -0.4989 | -0.3320 | -0.4703 | 0.2492 | -3.303 |
| 0.2916 | -0.6292 | -0.4100 | -0.6050 | 0.3464 | -4.152 |
| 0.3955 | -0.7109 | -0.4488 | -0.6931 | 0.4343 | -4.672 |
| 0.5022 | -0.7249 | -0.4407 | -0.7121 | 0.4905 | -4.759 |
| 0.5932 | -0.6846 | -0.4013 | -0.6735 | 0.5035 | -4.501 |
| 0.7095 | -0.5667 | -0.3165 | -0.5565 | 0.4626 | -3.754 |
| 0.7994 | -0.4330 | -0.2307 | -0.4202 | 0.3795 | -2.874 |
| 0.9023 | -0.2327 | -0.1169 | -0.2215 | 0.2205 | -1.553 |
| 308.15 K | | | | | |
| 0.0985 | -0.2487 | -0.1743 | -0.2372 | 0.1078 | -1.824 |
| 0.1999 | -0.4436 | -0.3110 | -0.4425 | 0.2192 | -3.167 |
| 0.2916 | -0.5700 | -0.3813 | -0.5661 | 0.3022 | -3.958 |
| 0.3955 | -0.6561 | -0.4151 | -0.6457 | 0.3767 | -4.413 |
| 0.5022 | -0.6801 | -0.4055 | -0.6603 | 0.4239 | -4.438 |
| 0.5932 | -0.6499 | -0.3674 | -0.6215 | 0.4341 | -4.143 |
| 0.7095 | -0.5415 | -0.2874 | -0.5093 | 0.3979 | -3.388 |
| 0.7994 | -0.4169 | -0.2079 | -0.3816 | 0.3258 | -2.548 |
| 0.9023 | -0.2270 | -0.1040 | -0.1986 | 0.1882 | -1.346 |
| 313.15 K | | | | | |
| 0.0985 | -0.2131 | -0.1624 | -0.2216 | 0.0948 | -1.714 |
| 0.1999 | -0.3871 | -0.2743 | -0.3934 | 0.1810 | -2.987 |
| 0.2916 | -0.5076 | -0.3364 | -0.5038 | 0.2492 | -3.728 |
| 0.3955 | -0.5961 | -0.3658 | -0.5743 | 0.3104 | -4.130 |
| 0.5022 | -0.6349 | -0.3565 | -0.5867 | 0.3490 | -4.105 |
| 0.5932 | -0.6130 | -0.3219 | -0.5502 | 0.3572 | -3.777 |
| 0.7095 | -0.5132 | -0.2501 | -0.4475 | 0.3271 | -3.014 |
| 0.7994 | -0.3957 | -0.1796 | -0.3328 | 0.2674 | -2.213 |
| 0.9023 | -0.2123 | -0.0884 | -0.1702 | 0.1534 | -1.131 |
| 318.15 K | | | | | |
| 0.0985 | -0.1836 | -0.1489 | -0.2040 | 0.0816 | -1.652 |
| 0.1999 | -0.3391 | -0.2424 | -0.3505 | 0.1492 | -2.861 |
| 0.2916 | -0.4561 | -0.2937 | -0.4446 | 0.2026 | -3.547 |
| 0.3955 | -0.5497 | -0.3169 | -0.5037 | 0.2502 | -3.889 |
| 0.5022 | -0.5919 | -0.3066 | -0.5110 | 0.2798 | -3.815 |
| 0.5932 | -0.5804 | -0.2753 | -0.4767 | 0.2854 | -3.461 |
| 0.7095 | -0.4888 | -0.2118 | -0.3839 | 0.2605 | -2.702 |
| 0.7994 | -0.3802 | -0.1506 | -0.2827 | 0.2121 | -1.943 |
| 0.9023 | -0.2086 | -0.0779 | -0.1517 | 0.1296 | -0.964 |
| 323.15 K | | | | | |
| 0.0985 | -0.1544 | -0.1380 | -0.1894 | 0.0712 | -1.559 |
| 0.1999 | -0.2893 | -0.2178 | -0.3165 | 0.1258 | -2.701 |
| 0.2916 | -0.4010 | -0.2531 | -0.3871 | 0.1626 | -3.337 |
| 0.3955 | -0.4979 | -0.2678 | -0.4315 | 0.1963 | -3.630 |
| 0.5022 | -0.5488 | -0.2550 | -0.4317 | 0.2159 | -3.513 |
| 0.5932 | -0.5461 | -0.2269 | -0.3996 | 0.2188 | -3.136 |
| 0.7095 | -0.4619 | -0.1763 | -0.3243 | 0.2033 | -2.378 |
| 0.7994 | -0.3606 | -0.1273 | -0.2421 | 0.1696 | -1.658 |
| 0.9023 | -0.1972 | -0.0680 | -0.1335 | 0.1083 | -0.785 |

the mixture is less compressible than an ideal solution. The most negative values occur at intermediate mole fractions suggesting strong ion-dipole and H-bonding interactions that lead to a compact, rigid structure resistant to compression. The decreasing magnitude of $K_{s,m}^E$ with increasing temperature confirms that these interactions are with thermal agitation [34].

In Fig. 6, the excess speed of sound $u^E$ exhibits positive deviations, especially near equimolar composition. This trend is characteristic of

**Table 4**
Coefficients, $A_i$ of equation (15) for $V_m^E$, $\kappa_s^E$, $K_{s,m}^E$, $u^E$, $\alpha_p^E$ and corresponding standard deviations, $\sigma$ for [BMIM][$BF_4$] + propyl acetate mixtures at temperatures, $T$/K = (298.15 – 323.15).

| $T$/K | $A_1$ | $A_2$ | $A_3$ | $\sigma(Y^E)$ |
|---|---|---|---|---|
| $10^6 \cdot V_m^E/m^3 \cdot mol^{-1}$ | | | | |
| 298.15 | -3.077 | 0.569 | -0.128 | 0.287 |
| 303.15 | -2.898 | 0.353 | -0.033 | 0.269 |
| 308.15 | -2.716 | 0.147 | 0.074 | 0.251 |
| 313.15 | -2.526 | -0.039 | 0.224 | 0.233 |
| 318.15 | -2.358 | -0.205 | 0.285 | 0.218 |
| 323.15 | -2.182 | -0.360 | 0.389 | 0.203 |
| $10^{10} \cdot \kappa_s^E/m^2 \cdot N^{-1}$ | | | | |
| 298.15 | -1.914 | 0.550 | 0.011 | 0.181 |
| 303.15 | -1.765 | 0.533 | 0.023 | 0.167 |
| 308.15 | -1.627 | 0.529 | 0.051 | 0.155 |
| 313.15 | -1.427 | 0.500 | 0.023 | 0.136 |
| 318.15 | -1.223 | 0.479 | -0.044 | 0.118 |
| 323.15 | -1.015 | 0.465 | -0.192 | 0.099 |
| $10^{14} \cdot K_{s,m}^E/m^5 \cdot N^{-1} \cdot mol^{-1}$ | | | | |
| 298.15 | -3.067 | 0.244 | 0.170 | 0.284 |
| 303.15 | -2.849 | 0.270 | 0.192 | 0.264 |
| 308.15 | -2.646 | 0.309 | 0.242 | 0.246 |
| 313.15 | -2.346 | 0.326 | 0.214 | 0.218 |
| 318.15 | -2.037 | 0.352 | 0.115 | 0.190 |
| 323.15 | -1.718 | 0.379 | -0.105 | 0.161 |
| $10^{-2} \cdot u^E/m \cdot s^{-1}$ | | | | |
| 298.15 | 2.258 | 0.785 | 0.005 | 0.215 |
| 303.15 | 1.959 | 0.674 | 0.012 | 0.187 |
| 308.15 | 1.695 | 0.560 | -0.006 | 0.161 |
| 313.15 | 1.394 | 0.445 | 0.016 | 0.132 |
| 318.15 | 1.113 | 0.335 | 0.080 | 0.105 |
| 323.15 | 0.856 | 0.238 | 0.208 | 0.081 |
| $10^3 \cdot \alpha_p^E/K^{-1}$ | | | | |
| 298.15 | -20.310 | 1.213 | -1.046 | 1.879 |
| 303.15 | -19.044 | 2.280 | -0.677 | 1.768 |
| 308.15 | -17.767 | 3.262 | -0.215 | 1.658 |
| 313.15 | -16.440 | 4.075 | 0.573 | 1.546 |
| 318.15 | -15.281 | 4.825 | 0.786 | 1.452 |
| 323.15 | -14.077 | 5.471 | 1.301 | 1.356 |

enhanced structural cohesion and reduced free volume due to tightly bound molecular complexes forming. The increase in $u^E$ supports the view that strong molecular associations, primarily electrostatic and H-bonding, enhance the propagation of sound through the medium [35, 36].

Fig. 7 reveals that the excess isobaric expansivity, $\alpha_p^E$ values are predominantly negative, particularly at intermediate compositions, reflecting a reduced thermal response of the system. This suggests that the molecular structure becomes more compact and less responsive to temperature-induced volume changes due to the formation of energetically stable interactions. As with other properties, the effect diminishes with increasing temperature, consistent with the disruption of structured networks [37].

### 3.2. Partial molar properties

The partial molar properties like partial molar volumes and partial molar isentropic compressibilities of the components, [BMIM][$BF_4$] and propyl acetate, in the mixture over the entire range of composition were determined using the following relations [38,39]

$$\overline{Y}_{m,1} = Y_m^E + Y_{m,1}^* + x_2 \left( \frac{\partial Y_m^E}{\partial x_1} \right)_{T,P} \quad (17)$$

$$\overline{Y}_{m,2} = Y_m^E + Y_{m,2}^* - x_1 \left( \frac{\partial Y_m^E}{\partial x_1} \right)_{T,P} \quad (18)$$

where $Y_{m,1}^*$ and $Y_{m,2}^*$ are the molar properties of pure components in the

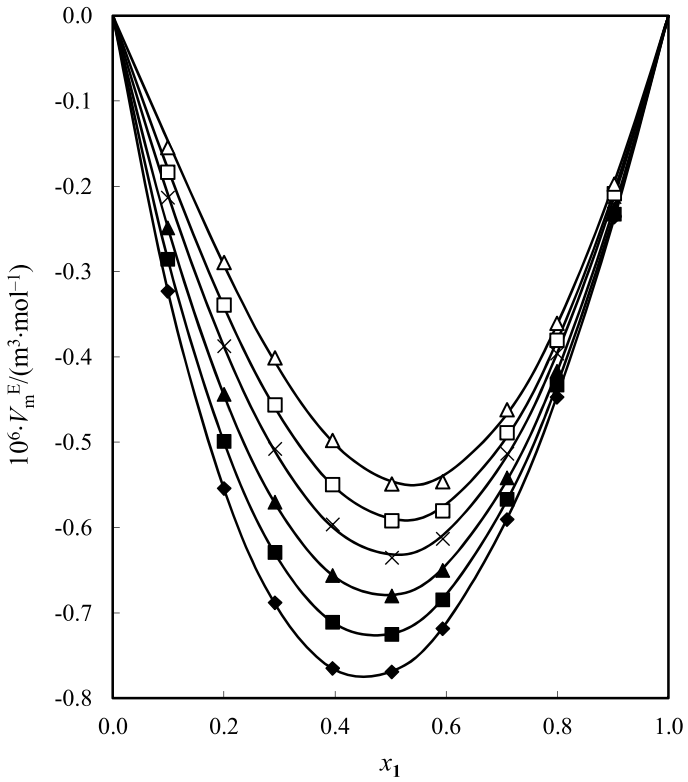


**Fig. 1.** Plots of excess molar volume, $V_m^E$ *vs.* mole fraction, $x_1$ for [BMIM][$BF_4$] + propyl acetate binary mixtures at temperatures, $T$/K = 298.15, ◆; At $T$/K = 303.15, ■; $T$/K = 308.15, ▲; $T$/K = 313.15, ×; $T$/K = 318.15, □; $T$/K = 323.15, Δ. The points represent experimental values and lines represent values calculated from equation (15).

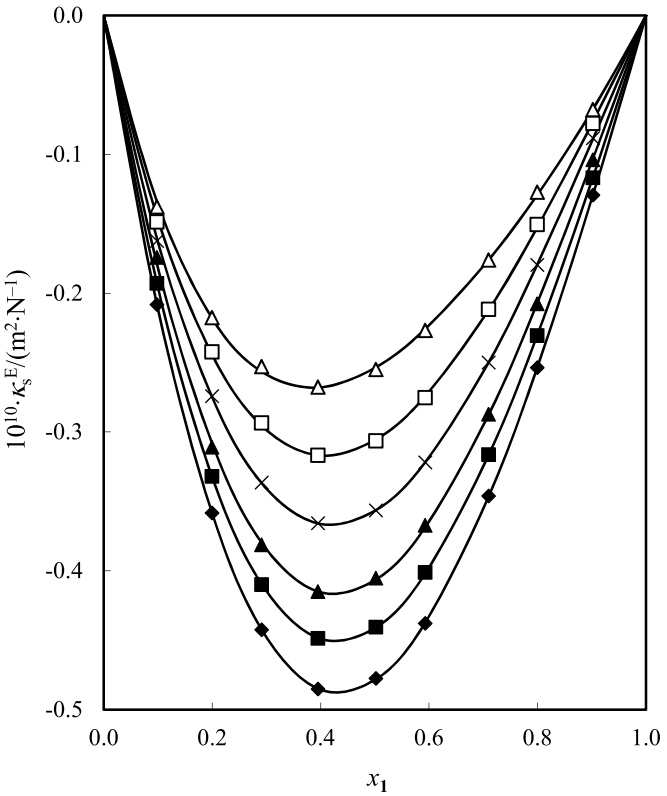


**Fig. 2.** Excess isentropic compressibilities, $\kappa_m^E$ with mole fraction $x_1$ for [BMIM][$BF_4$] + propyl acetate binary mixtures at temperatures. The legends are the same as given in Fig. 1.

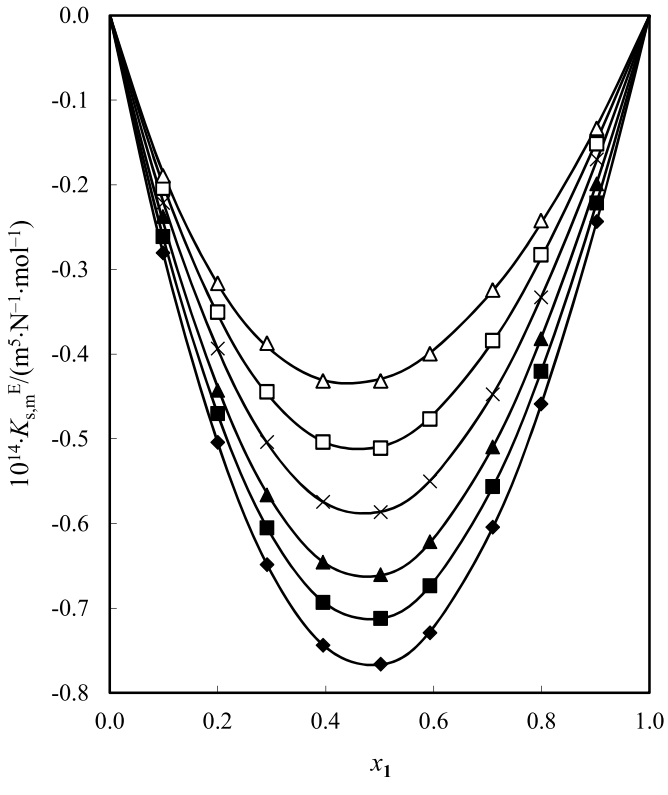


**Fig. 3.** Excess molar isentropic compressibilities, $K_{s,m}^E$ with mole fraction $x_1$ for [BMIM][$BF_4$] + propyl acetate binary mixtures at temperatures. The legends are the same as given in Fig. 1.

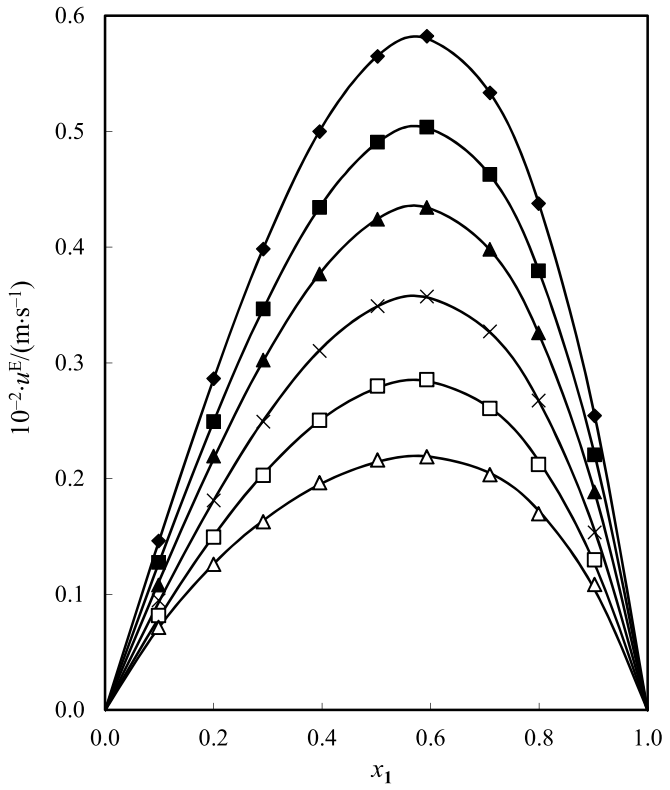


**Fig. 4.** Excess speeds of sound, $u^{E}$ with mole fraction $x_1$ for [BMIM][$BF_4$] + propyl acetate binary mixtures at temperatures. The legends are the same as given in Fig. 1.

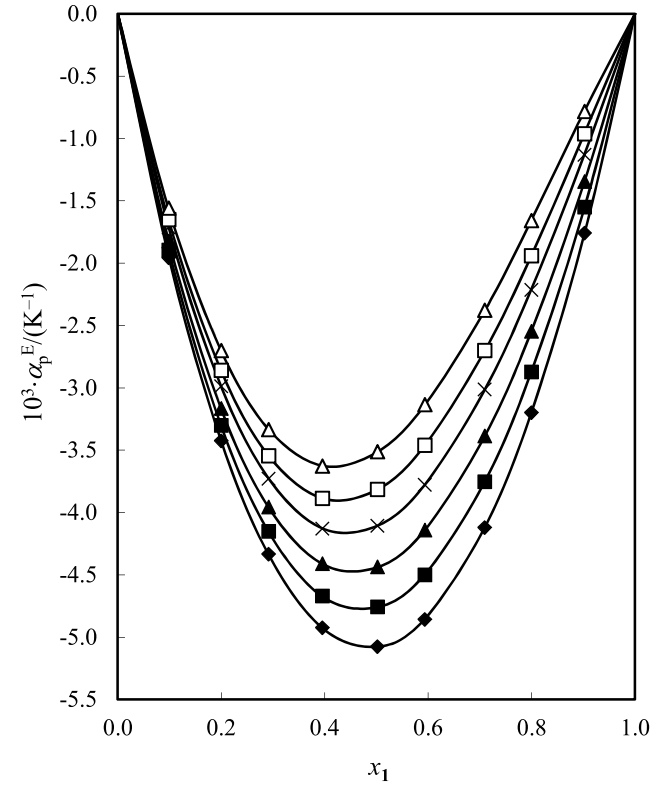


**Fig. 5.** Excess isobaric thermal expansivity, $\alpha_p^{E}$ with mole fraction $x_1$ for [BMIM][$BF_4$] + propyl acetate binary mixtures at temperatures. The legends are the same as given in Fig. 1.

mixtures. The derivative, $\left(\frac{\partial Y_m^E}{\partial x_1}\right)_{T,P}$ in equations (17) and (18) is obtained from the differentiation of equation (15) and substituting its value resulted in equations for $\overline{Y}_{m,1}$ and $\overline{Y}_{m,2}$

$$\overline{Y}_{m,1} = Y_m^E + Y_{m,1}^* + x_2^2\sum_{i=0}^{n}A_i(1-2x_1)^i - 2x_1x_2\sum_{i=0}^{n}A_i(1-2x_1)^{i-1} \quad (19)$$

$$\overline{Y}_{m,2} = Y_m^E + Y_{m,2}^* - x_1^2\sum_{i=0}^{n}A_i(1-2x_1)^i + 2x_1^2x_2\sum_{i=1}^{n}A_i(1-2x_1)^{i-1} \quad (20)$$

The values of $\overline{V}_{m,1}$, $\overline{V}_{m,2}$, $\overline{K}_{s,m,1}$ and $\overline{K}_{s,m,2}$ as functions of the mole fraction, $x_1$ for these mixtures at each temperature are recorded in Tables 5 and 6. The values of $\overline{Y}_{m,1}^E$ and $\overline{Y}_{m,2}^E$ were calculated by using the following equations [40,41]

$$\overline{Y}_{m,i}^E = Y_m^E + (1-x_i)\left(\frac{\partial Y_m^E}{\partial x_i}\right) \quad (21)$$

The graphical representation of $\overline{V}_{m,1}^E$ and $\overline{V}_{m,2}^E$; as well as $\overline{K}_{s,m,1}^E$ and $\overline{K}_{s,m,2}^E$ in relation to composition and temperature are illustrated in Figs. 6 and 7, respectively. Fig. 6 indicates that the values of $\overline{V}_{m,1}^E$ and $\overline{V}_{m,2}^E$ values for these mixtures remain negative throughout the entire composition range at all temperatures. This suggests that the molar volume of each constituent within the mixture is diminished compared to their molar volumes in the pure state, indicating a reduction in volume upon the amalgamation of [BMIM][$BF_4$] with propyl acetates. The negative $\overline{V}_{m,1}^E$ and $\overline{V}_{m,2}^E$ indicate significant solute-solvent interactions among [BMIM][$BF_4$] and propyl acetate molecules, characterised by robust ion-dipole and hydrogen bonding interactions. These interactions arise from the ions formed by the ionic liquid, [$BMIM^+$] and [$BF_4^-$], and dipoles of propyl acetate molecules. The observed trends in $\overline{V}_{m,1}^E$ and $\overline{V}_{m,2}^E$ values further reinforce the conclusions derived from $V_m^E$ values.

Fig. 7 indicates that the values of $\overline{K}_{s,m,1}^E$ and $\overline{K}_{s,m,2}^E$ are negative for these mixtures across the entire composition range at each temperature. This suggests that the $K_{s,m}$ of each component within the mixture is diminished compared to their $K_{s,m}$ in pure state, indicating a reduction in compressibility when IL are mixed with propyl acetates. The negative $\overline{K}_{s,m,1}^E$ and $\overline{K}_{s,m,2}^E$ values indicate significant interactions between solute and solvent specifically between [BMIM][$BF_4$] and propyl acetate molecules. The observed trends seen in $\overline{K}_{s,m,1}^E$ and $\overline{K}_{s,m,2}^E$ values provide additional support for the conclusions derived from $\kappa_s^E$ and $K_{s,m}^E$ values.

The partial molar properties, $\overline{Y}_{m,1}^{\circ}$ of [BMIM][$BF_4$] at infinite dilution ($x_1 = 0$) in propyl acetate, and $\overline{Y}_{m,1}^{\circ}$ of propyl acetate at infinite dilution ($x_2 = 0$) in [BMIM][$BF_4$]. Therefore, $\overline{Y}_{m,1}^{\circ}$ is obtained by setting $x_1 = 0$, by means of equation

$$\overline{Y}_{m,1}^{\circ} = Y_{m,1}^* + \sum_{i=0}^{n}A_i(-1)^i \quad (22)$$

Similarly, $\overline{Y}_{m,1}^{\circ}$ is obtained by setting $x_2$=0, by means of equation

$$\overline{Y}_{m,2}^{\circ} = Y_{m,2}^* + \sum_{i=0}^{n}A_i \quad (23)$$

The excess partial molar properties at infinite dilution, $\overline{Y}_{m,i}^{\circ E}$ for each component in binary mixtures were evaluated through relations

$$\overline{Y}_{m,1}^{\circ E} = \overline{Y}_{m,1}^{\circ} - Y_{m,1}^* \quad (24)$$

$$\overline{Y}_{m,2}^{\circ E} = \overline{Y}_{m,2}^{\circ} - Y_{m,2}^* \quad (25)$$

The values of $\overline{V}_{m,1}^{\circ}$, $V_{m,1}^*$, $\overline{V}_{m,1}^{\circ E}$, $\overline{V}_{m,2}^{\circ}$, $V_{m,2}^*$ and $\overline{V}_{m,2}^{\circ E}$; and $\overline{K}_{s,m,1}^{\circ}$, $K_{s,m,1}^*$,

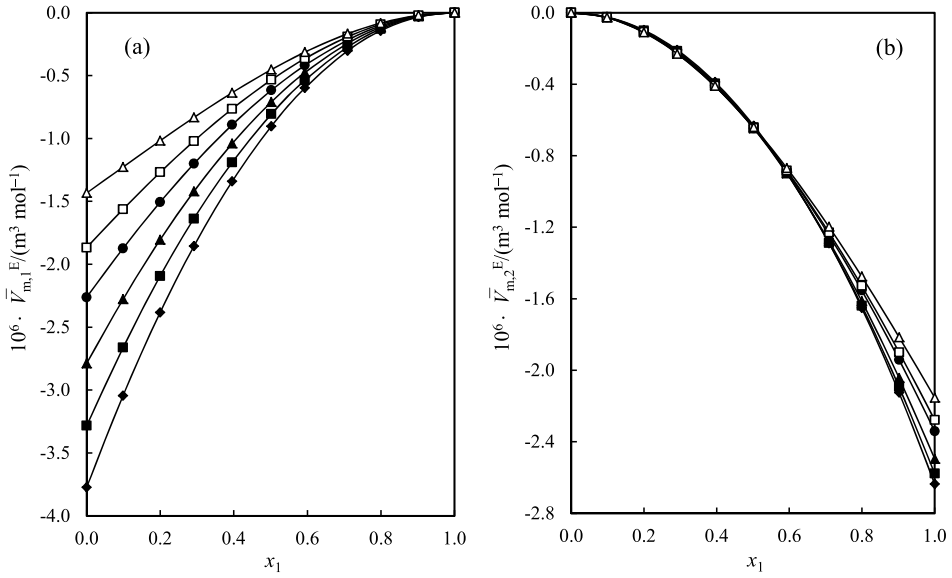


**Fig. 6.** Variations of excess partial molar volume, $\overline{V}_{m,1}^{E}$ and $\overline{V}_{m,2}^{E}$, of (a) [BMIM][$BF_4$] and (b) propyl acetate, respectively, with mole fraction, $x_1$ of [BMIM][$BF_4$] for [BMIM][$BF_4$] + propyl acetate binary mixtures at temperatures, $T$/K = 298.15, ◆; At $T$/K = 303.15, ■; $T$/K = 308.15, ▲; $T$/K = 313.15, ×; $T$/K = 318.15, □; $T$/K = 323.15, Δ.

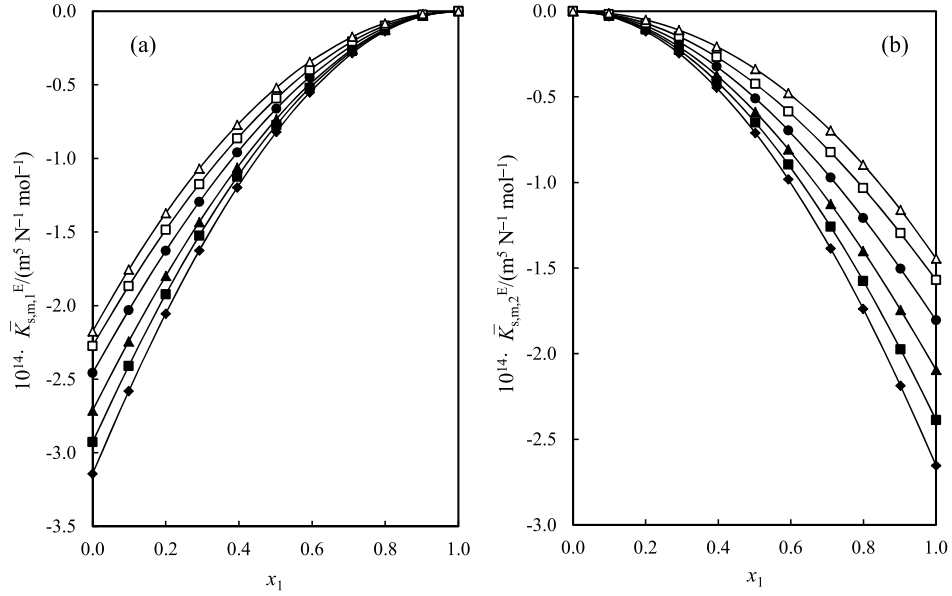


**Fig. 7.** Variations of excess partial molar compressibilities, $\overline{K}_{s,m,1}^{E}$ and $\overline{K}_{s,m,2}^{E}$, of (a) [BMIM][$BF_4$] and (b) propyl acetate, respectively, with mole fraction, $x_1$ of [BMIM][$BF_4$] for [BMIM][$BF_4$] + propyl acetate binary mixtures at temperatures. The legends are the same as given in Fig. 6.

$\overline{K}_{s,m,1}^{\circ E}$, $\overline{K}_{s,m,1}^{\circ}$, $K_{s,m,2}^{*}$ and $\overline{K}_{s,m,2}^{\circ E}$ for the binary mixtures at each investigated temperature are listed in Tables 7 and 8, respectively.

The excess partial molar properties at infinite dilution provide valuable insight into the solvation behaviour and strength and nature of solute-solvent interactions within binary mixtures. An examination of Table 5 reveals that the values of $\overline{V}_{m,1}^{\circ E}$ and $\overline{V}_{m,2}^{\circ E}$ are consistently negative across all mixtures throughout the complete temperature range. This suggests that the volumes of each component within the mixture are diminished compared to their volumes in the pure form. The observed reduction in volumes further indicates that the interactions between [BMIM][$BF_4$] and propyl acetate are more robust than those found in the pure components. The values of $\overline{V}_{m,1}^{\circ E}$ and $\overline{V}_{m,2}^{\circ E}$ decreases with an increase in temperature of the mixture, further supporting the observed trends for $V_m^E$ values for those binary systems.

An examination of Table 6 reveals that the values of $\overline{K}_{s,m,1}^{\circ,E}$ and $\overline{K}_{s,m,2}^{\circ,E}$ remain negative throughout the entire temperature spectrum for all the binary mixtures under investigation. The values of $\overline{K}_{s,m,1}^{\circ,E}$ and $\overline{K}_{s,m,2}^{\circ,E}$ depends on both structural and geometrical factors [42–44]. The separation of bonds during the mixing of components results in structural compressibility and enhanced association. Conversely, the amalgamation of the mixture's components induces geometrical compressibility, culminating in a reduction of volume and a decrease in the average intermolecular distance. The recorded negative values $\overline{K}_{s,m,1}^{\circ,E}$ and $\overline{K}_{s,m,2}^{\circ,E}$ suggest that the geometrical compressibility factor plays a predominant role in these mixtures. Furthermore, the values of $\overline{K}_{s,m,1}^{\circ,E}$ and $\overline{K}_{s,m,2}^{\circ,E}$

**Table 5**
Partial molar volumes, $\overline{V}_{m,1}$ and $\overline{V}_{m,2}$, of [BMIM][$BF_4$] and propyl acetate, respectively, at each mole fraction, $x_1$ for [BMIM][$BF_4$] + propyl acetate mixtures at temperatures, $T$/K = (298.15 – 323.15).

| $x_1$ | $T$/K | | | | | |
|---|---|---|---|---|---|---|
| | 298.15 | 303.15 | 308.15 | 313.15 | 318.15 | 323.15 |
| $10^6 \cdot \overline{V}_{m,1}$/$m^3 \cdot mol^{-1}$ | | | | | | |
| 0.0000 | 184.767 | 185.824 | 186.887 | 187.966 | 188.945 | 189.949 |
| 0.0985 | 185.494 | 186.445 | 187.398 | 188.354 | 189.249 | 190.156 |
| 0.1999 | 186.157 | 187.014 | 187.871 | 188.723 | 189.544 | 190.366 |
| 0.2916 | 186.684 | 187.470 | 188.255 | 189.027 | 189.792 | 190.550 |
| 0.3955 | 187.198 | 187.917 | 188.635 | 189.337 | 190.048 | 190.747 |
| 0.5022 | 187.637 | 188.302 | 188.966 | 189.612 | 190.279 | 190.931 |
| 0.5932 | 187.941 | 188.571 | 189.200 | 189.810 | 190.448 | 191.070 |
| 0.7095 | 188.237 | 188.835 | 189.432 | 190.011 | 190.621 | 191.216 |
| 0.7994 | 188.396 | 188.978 | 189.559 | 190.123 | 190.720 | 191.301 |
| 0.9023 | 188.506 | 189.077 | 189.648 | 190.203 | 190.790 | 191.363 |
| 1.0000 | 188.540 | 189.108 | 189.676 | 190.229 | 190.813 | 191.383 |
| $10^6 \cdot \overline{V}_{m,2}$/$m^3 \cdot mol^{-1}$ | | | | | | |
| 0.0000 | 115.687 | 116.430 | 117.183 | 117.951 | 118.732 | 119.527 |
| 0.0985 | 115.664 | 116.405 | 117.158 | 117.924 | 118.705 | 119.499 |
| 0.1999 | 115.590 | 116.329 | 117.079 | 117.843 | 118.623 | 119.416 |
| 0.2916 | 115.479 | 116.214 | 116.962 | 117.724 | 118.504 | 119.297 |
| 0.3955 | 115.299 | 116.033 | 116.779 | 117.542 | 118.322 | 119.117 |
| 0.5022 | 115.055 | 115.788 | 116.535 | 117.304 | 118.086 | 118.886 |
| 0.5932 | 114.796 | 115.532 | 116.284 | 117.062 | 117.849 | 118.658 |
| 0.7095 | 114.398 | 115.141 | 115.905 | 116.706 | 117.502 | 118.329 |
| 0.7994 | 114.036 | 114.791 | 115.570 | 116.397 | 117.203 | 118.051 |
| 0.9023 | 113.561 | 114.336 | 115.139 | 116.009 | 116.832 | 117.712 |
| 1.0000 | 113.051 | 113.851 | 114.687 | 115.610 | 116.454 | 117.373 |

**Table 6**
Partial molar isentropic compressibilities, $\overline{K}_{s,m,1}$ and $\overline{K}_{s,m,2}$ [BMIM][$BF_4$] and propyl acetate, respectively, as functions of mole fraction, $x_1$ of [BMIM][$BF_4$] for [BMIM][$BF_4$] + propyl acetate mixtures at temperatures, $T$/K = (298.15 – 323.15).

| $x_1$ | $T$/K | | | | | |
|---|---|---|---|---|---|---|
| | 298.15 | 303.15 | 308.15 | 313.15 | 318.15 | 323.15 |
| $10^{14} \cdot \overline{K}_{s,m,1}$/ $m^5\ N^{-1}\ mol^{-1}$ | | | | | | |
| 0.0000 | 3.280 | 3.634 | 3.988 | 4.386 | 4.716 | 4.964 |
| 0.0985 | 3.842 | 4.152 | 4.458 | 4.812 | 5.124 | 5.384 |
| 0.1999 | 4.367 | 4.638 | 4.902 | 5.216 | 5.505 | 5.767 |
| 0.2916 | 4.796 | 5.036 | 5.269 | 5.548 | 5.816 | 6.071 |
| 0.3955 | 5.225 | 5.436 | 5.640 | 5.884 | 6.126 | 6.367 |
| 0.5022 | 5.601 | 5.788 | 5.969 | 6.182 | 6.399 | 6.620 |
| 0.5932 | 5.869 | 6.039 | 6.205 | 6.395 | 6.592 | 6.795 |
| 0.7095 | 6.137 | 6.291 | 6.443 | 6.611 | 6.785 | 6.965 |
| 0.7994 | 6.285 | 6.431 | 6.577 | 6.731 | 6.892 | 7.057 |
| 0.9023 | 6.389 | 6.530 | 6.671 | 6.817 | 6.967 | 7.120 |
| 1.0000 | 6.422 | 6.561 | 6.701 | 6.844 | 6.991 | 7.139 |
| $10^{14} \cdot \overline{K}_{s,m,2}$/ $m^5\ N^{-1}\ mol^{-1}$ | | | | | | |
| 0.0000 | 9.654 | 10.140 | 10.669 | 11.223 | 11.832 | 12.469 |
| 0.0985 | 9.625 | 10.114 | 10.644 | 11.202 | 11.815 | 12.456 |
| 0.1999 | 9.537 | 10.032 | 10.570 | 11.137 | 11.762 | 12.418 |
| 0.2916 | 9.407 | 9.914 | 10.462 | 11.044 | 11.684 | 12.358 |
| 0.3955 | 9.206 | 9.730 | 10.296 | 10.900 | 11.564 | 12.262 |
| 0.5022 | 8.942 | 9.490 | 10.080 | 10.714 | 11.407 | 12.131 |
| 0.5932 | 8.671 | 9.245 | 9.863 | 10.527 | 11.246 | 11.990 |
| 0.7095 | 8.268 | 8.882 | 9.544 | 10.252 | 11.008 | 11.772 |
| 0.7994 | 7.914 | 8.565 | 9.268 | 10.015 | 10.799 | 11.573 |
| 0.9023 | 7.466 | 8.166 | 8.925 | 9.719 | 10.535 | 11.309 |
| 1.0000 | 7.000 | 7.752 | 8.574 | 9.418 | 10.262 | 11.024 |

exhibit a decline as temperature rises, resulting in a reduction in the volume of the mixture. The observed trends provide additional validation for the conclusions derived from the variations in the values of $\kappa_s^E$, $L_f^E$, $u^E$and $K_{s,m}^E$ pertaining to these binary mixtures.

**Table 7**
The values of $\overline{V}^{\circ}_{m,1}$ $\overline{V}^{\circ}_{m,1}$, $V^{*}_{m,1}$, $\overline{V}^{*E}_{m,1}$, $\overline{V}^{\circ}_{m,2}$, $V^{*}_{m,2}$ and $\overline{V}^{*E}_{m,2}$ for the components for [BMIM][$BF_4$] + propyl acetate mixtures at temperatures, $T$/K = (293.15 – 318.15).

| $T$/K | $10^6 \cdot \overline{V}^{\circ}_{m,1}$ | $10^6 \cdot V^{*}_{m,1}$ | $10^6 \cdot \overline{V}^{E}_{m,1}$ | $10^6 \cdot \overline{V}^{\circ}_{m,2}$ | $10^6 \cdot V^{*}_{m,2}$ | $10^6 \cdot \overline{V}^{E}_{m,2}$ |
|---|---|---|---|---|---|---|
| | $m^3 \cdot mol^{-1}$ | | | | | |
| 298.15 | 184.77 | 188.54 | -3.77 | 113.05 | 115.69 | -2.64 |
| 303.15 | 185.82 | 189.11 | -3.28 | 113.85 | 116.43 | -2.58 |
| 308.15 | 186.89 | 189.68 | -2.79 | 114.69 | 117.18 | -2.50 |
| 313.15 | 187.97 | 190.23 | -2.26 | 115.61 | 117.95 | -2.34 |
| 318.15 | 188.94 | 190.81 | -1.87 | 116.45 | 118.73 | -2.28 |
| 323.15 | 189.95 | 191.38 | -1.43 | 117.37 | 119.53 | -2.15 |

## 4. Calculation of excess molar volume ($V_m^E$) with the PFP theory

A number of articles were found in the literature, reporting the prediction of $V_m^E$ of the liquid mixtures with IL as one component by means of Prigogine-Flory-Patterson (PFP) statistical theory. In the PFP theory, $V_m^E$ is divided into three contribution terms: (i) the free volume, $V_m^E$(fv), (ii) the characteristic pressure, $V_m^E$(ip), and (iii) the energy of interaction, $V_m^E$(int). These three contributions together can be expressed as term I, II and III on right hand side, respectively, in the following equation

$$\frac{V_m^E}{x_1V_1^* + x_2V_2^*} = \frac{(\tilde{V}^{1/3} - 1)\tilde{V}^{2/3}}{[(4/3)\tilde{V}^{-1/3} - 1]}\Psi_1\theta_2\left(\frac{\chi_{12}}{P_1^*}\right) - \frac{(V_1 - V_2)^2\left[(14/9)\tilde{V}^{-\frac{1}{3}} - 1\right]\Psi_1\Psi_2}{\left[\left(\frac{4}{3}\right)\tilde{V}^{-\frac{1}{3}} - 1\right)\tilde{V}} + \frac{(\tilde{V}_1 - \tilde{V}_2)(P_1^* - P_2^*)}{P_1^*\Psi_2 + P_2^*\Psi_1}\Psi_1\Psi_2 \quad (26)$$

Here $x_i$, $P_i^*$, $V_i^*$, $\tilde{V}_i$, $\theta_i$ and$\Psi_i$ are the mole fraction, characteristic pressure, characteristic volume, reduced volume, segment fraction and contact energy fraction of $i^{th}$ component, respectively, outlined previously [45–48].

The term $\chi_{12}$ in equation (26) is the Flory's contact interaction parameter. The parameters of the pure components used in the calculation of $V_m^E$ by PFP theory are reported in Table 9. The only adjustable parameter of the PFP theory, $\chi_{12}$is calculated from experimental $V_m^E$ values (at $x_1$ = 0.5) when the values of experimental excess molar enthalpy, $H_m^E$ are not available. The values of $\chi_{12}$for these mixtures are positive. Fig. 8 shows the comparison between $V_{Exp}^E$ and $V_{PFP}^E$ for the binary mixtures across entire mole fraction range at studied temperatures. The values of the PFP contributions, $V_m^E$(fv), $V_m^E$(ip), and $V_m^E$(int) to $V_{PFP}^E$ at equimolar composition and $V_{Exp}^E$ and $V_{PFP}^E$ are summarized in Table 10.

Table 10 presents the experimental and PFP theory-predicted values of excess molar volume for non-equimolar mixtures of [BMIM][$BF_4$] and propyl acetate across the temperature range of 298.15-323.15 K. The negative $V_m^E$ values indicates significant molecular interactions and volume contraction upon mixing, suggesting strong specific interactions such as ion-dipole forces and H-bonding between the IL and ester. The close agreement between $V_{Exp}^E$ and $V_{PFP}^E$ values demonstrate the reliability of the PFP model in describing the volumetric behaviour of such mixtures. The PFP contributions, *viz.*, interaction (int), free volume (fv) and internal pressure (ip) reveal that the negative $V_m^E$ arises mainly from the negative internal pressure term, partially compensated by positive interaction and free volume effects. These findings underline that molecular interactions dominate the volumetric behaviour, while the

**Table 8**

The values of $\overline{K}^{\circ}_{s,m,1}$, $K^{*}_{s,m,1}$, $\overline{K}^{\circ E}_{s,m,1}$, $\overline{K}^{\circ}_{s,m,2}$, $K^{*}_{s,m,2}$ and $\overline{K}^{\circ E}_{s,m,2}$ for the components for [BMIM][$BF_4$] + propyl acetate mixtures at temperatures, $T$/K = (298.15 – 323.15).

| $T$/K | $10^{14}\cdot\overline{K}^{\circ}_{s,m,1}$ | $10^{14}\cdot K^{*}_{s,m,1}$ | $10^{14}\cdot\overline{K}^{\circ E}_{s,m,1}$ | $10^{14}\cdot\overline{K}^{\circ}_{s,m,2}$ | $10^{14}\cdot K^{*}_{s,m,2}$ | $10^{14}\cdot\overline{K}^{\circ E}_{s,m,2}$ |
|---|---|---|---|---|---|---|
| | $m^5\cdot N^{-1}\cdot mol^{-1}$ | | | | | |
| 293.15 | 3.280 | 6.422 | -3.142 | 7.000 | 9.654 | -2.653 |
| 298.15 | 3.634 | 6.561 | -2.927 | 7.752 | 10.140 | -2.388 |
| 303.15 | 3.988 | 6.701 | -2.713 | 8.574 | 10.669 | -2.095 |
| 308.15 | 4.386 | 6.844 | -2.458 | 9.418 | 11.223 | -1.805 |
| 313.15 | 4.716 | 6.991 | -2.275 | 10.262 | 11.832 | -1.570 |
| 318.15 | 4.964 | 7.139 | -2.175 | 11.024 | 12.469 | -1.444 |

**Table 9**

The values of reduced volume, $\widetilde{V}$, characteristic volume, $V^*$, characteristic pressure, $P^*$, characteristic temperature, $T^*$, isothermal compressibility, $\kappa_T$, isentropic compressibility, $\kappa_s$, and thermal expansion coefficient, $\alpha$ of pure liquids at temperatures, $T$/K = (298.15 to 323.15) K.

| $T$/K | $\widetilde{V}$ | $10^{6}\cdot V^*$/ $m^3.mol^{-1}$ | $10^{-8}\cdot P^*$/ $J\cdot cm^{-3}$ | $T^*$/K | $10^{10}\cdot\kappa_T$ / $m^2\cdot N^{-1}$ | $10^{10}\cdot\kappa_s$/ $m^2\cdot N^{-1}$ | $10^{-4}\cdot\alpha/K^{-1}$ | $C_p$/J·mol$^{-1}$ |
|---|---|---|---|---|---|---|---|---|
| [BMIM][$BF_4$] | | | | | | | | |
| 298.15 | 1.1598 | 162.56 | 6.082 | 7172 | 3.963 | 3.406 | 12.479 | 364.8 [20] |
| 303.15 | 1.1624 | 162.69 | 6.111 | 7202 | 4.035 | 3.470 | 12.558 | 367.2 [20] |
| 305.15 | 1.1631 | 163.08 | 6.060 | 7298 | 4.093 | 3.533 | 12.637 | 369.5 [20] |
| 313.15 | 1.1662 | 163.12 | 6.106 | 7311 | 4.171 | 3.598 | 12.718 | 371.9 [20] |
| 318.15 | 1.1688 | 163.26 | 6.132 | 7341 | 4.246 | 3.664 | 12.799 | 374.3 [20] |
| 323.15 | 1.1696 | 163.63 | 6.085 | 7429 | 4.308 | 3.730 | 12.881 | 376.6 [20] |
| Propyl acetate | | | | | | | | |
| 298.15 | 1.3033 | 88.763 | 5.785 | 4598 | 11.248 | 8.345 | 7.652 | 196.1 [21] |
| 303.15 | 1.3089 | 88.954 | 5.740 | 4624 | 11.699 | 8.709 | 7.681 | 197.4 [21] |
| 305.15 | 1.3144 | 89.152 | 5.689 | 4650 | 12.180 | 9.105 | 7.711 | 198.9 [21] |
| 313.15 | 1.3200 | 89.356 | 5.637 | 4676 | 12.680 | 9.515 | 7.741 | 200.3 [21] |
| 318.15 | 1.3256 | 89.568 | 5.577 | 4703 | 13.220 | 9.965 | 7.771 | 201.8 [21] |
| 323.15 | 1.3312 | 89.786 | 5.518 | 4729 | 13.778 | 10.432 | 7.801 | 203.4 [21] |

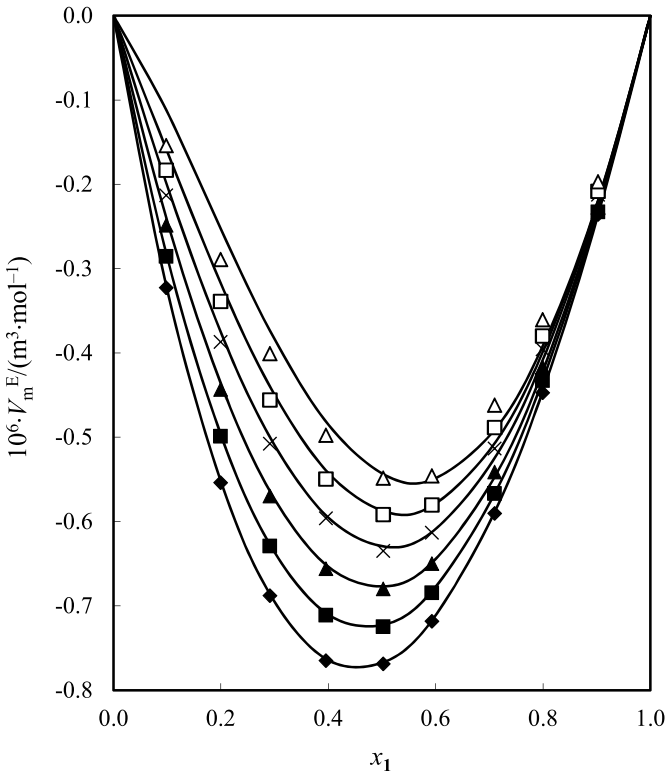


**Fig. 8.** Plots of excess molar volume, $V^E_m$ *vs.* mole fraction, $x_1$ of [BMIM][$BF_4$] for [BMIM][$BF_4$] + propyl acetate binary mixtures at temperatures, $T$/K = 298.15, ◆; At $T$/K = 303.15, ■; $T$/K = 308.15, ▲; $T$/K = 313.15, ×; $T$/K = 318.15, □; $T$/K = 323.15, Δ. The points represent experimental $V^E_m$ values and lines represent $V^E_m$ values calculated from PFP theory.

structural packing and free volume effects play secondary roles.

## 5. Modelling

### 5.1. Correlation of experimental data using Jouyban-Acree model

The Jouyban-Acree model [14,15] has been used to correlate the $\rho$ and $u$ data of these [BMIM][$BF_4$] + propyl acetate mixtures by means of the equation

$$\ln Y_T = x_1 \ln Y_{1,T} + x_2 \ln Y_{2,T} + j_0\left[\frac{x_1x_2}{T}\right] + j_1\left[\frac{x_1x_2(x_1-x_2)}{T}\right] + j_2\left[\frac{x_1x_2(x_1-x_2)^2}{T}\right] \quad (26a)$$

where $Y$ represents ~~is~~ the value of the $\rho$ or $u$ of the binary mixture at temperature, $T$. The coefficients $j_0$, $j_1$ and $j_2$ have been derived through the process of regressing $\ln Y_T - (x_1 \ln Y_{1,T} + x_2 \ln Y_{2,T})$ against $x_1x_2/T$, $x_1x_2(x_1 - x_2)/T$, and $x_1x_2(x_1 - x_2)^2/T$ employing multiple regression analysis *via* the matrix method. In order to assess the efficacy of the Jouyban-Acree model to correlating $\rho$ and $u$ data, one must consider the standard deviation of regression, $\sigma$, computed via equation (16), alongside the $r^2$ values for the regression and the average absolute percentage deviations, *AAPD* values, are derived from the specified equations

$$r^2 = 1 - \frac{\sum_{i=1}^{m}\left(Y_i^{exp.} - Y_i^{cal.}\right)^2}{\sum_{i=1}^{m}\left(Y_i^{exp.} - \overline{Y}_i\right)^2} \quad (27)$$

$$AAPD = \frac{100}{m}\sum_{i=1}^{m}\left|\frac{Y_i^{exp.} - Y_i^{cal.}}{Y_i^{exp.}}\right| \quad (28)$$

where $m$ is the number of data points, $\overline{Y}$ refers to the mean value of the respective property; superscript, *exp.* refers to experimental value and

**Table 10**
Values of $\chi_{12}$, $\theta_2$, experimental and calculated $V_m^E$ (using PFP theory) and three PFP contributions at near equimolar composition at temperatures, $T$/K = (298.15 to 323.15).

| $T$/K | $\theta_2$ | $10^{-8}\cdot\chi_{12}$/J·mol$^{-1}$ | $10^6\cdot V_m^E$ /m$^3$·mol$^{-1}$ | | | | |
|---|---|---|---|---|---|---|---|
| | | | Exp | PFP | PFP contribution to $V_m^E$ | | |
| | | | | | int | Fv | ip |
| 298.15 | 0.3984 | 0.185 | -1.4144 | -1.4106 | 0.315 | -0.877 | -0.204 |
| 303.15 | 0.3986 | 0.257 | -1.4551 | -1.4504 | 0.448 | -0.910 | -0.260 |
| 308.15 | 0.3986 | 0.317 | -1.4995 | -1.4954 | 0.568 | -0.973 | -0.272 |
| 313.15 | 0.3989 | 0.392 | -1.5474 | -1.5433 | 0.721 | -1.000 | -0.350 |
| 318.15 | 0.3992 | 0.461 | -1.5880 | -1.5831 | 0.871 | -1.035 | -0.424 |
| 323.15 | 0.3992 | 0.518 | -1.6376 | -1.6327 | 1.008 | -1.100 | -0.451 |

superscript, *cal.* refers to model calculated value. The values of $j_i$ coefficient, standard deviations, $\sigma$, $r^2$ and *AAPD* values for [BMIM][$BF_4$] + propyl acetate mixtures are listed in Tables 9 and 10.

The scrutiny of results given in Tables 9 and 10 displays that the Jouyben-Acree model correlates the experimental data well with very low $\sigma$ and *AAPD* values; and $r^2$ values are almost equal to 1, signifying an excellent agreement with the experimental $\rho$ and $u$ data of these mixtures at each studied temperature.

### 5.2. PC-SAFT EoS for computing liquid density

According to PC-SAFT EoS, the Helmholtz energy is expressed as

$$A = A^{ig} + A^{hc} + A^{disp} + A^{assoc} \tag{29}$$

where the different terms of the above equation, $A^{ig}$, $A^{hc}$, $A^{disp}$ and $A^{assoc}$ are related to the ideal gas term, a hard-chain contribution, London forces, and the association term, respectively. Each of the above contributions has been widely discussed in the literature [16,17].

The PC-SAFT equation of state requires five parameters for each pure substance: segment diameter, number of segments, energy parameter, effective volume related to the association, and energy parameter related to the association. These parameters are represented by $\sigma$, $m$, $\varepsilon$, $\kappa^{AB}$ and $\varepsilon^{AB}$. The last two parameters ($\kappa^{AB}$ and $\varepsilon^{AB}$) are set to zero if the substance doesn't associate. We have set this parameter to zero for a fully predictive model in the compute of density in multicomponent mixtures.

According to the literature [49,50], an association scheme is needed to account for the interactions among the cation and anion of ionic liquid. A 2B scheme with a positive and a negative site would be suitable for modelling the properties of an ionic liquid. This scheme was used by Shaahmadi *et al.* [49], who used the cubic plus association (CPA) model. On the other hand, propyl acetate doesn't self-associate; it can form associations with molecules that can donate hydrogen protons due to the presence of lone electron pairs on its oxygen atoms. Therefore, in the present study, we used a scheme with two negative sites for the propyl acetate. The PC-SAFT parameters for the ionic liquid were fitted to the experimental data of liquid density at atmospheric pressure published in our work, using the objective function expressed as

$$OF\left(m, \sigma, \frac{\varepsilon}{k_B}, \frac{\varepsilon^{AB}}{k_B}, k^{AB}\right) = \left(\frac{\rho_i^{calc} - \rho_i^{exp\,2}}{\rho_i^{exp}}\right) \tag{30}$$

where N is the number of experimental density data, *exp*, is related to the experimental value, while *calc*, is related to the theoretical value obtained with PC-SAFT EoS. For the case of propyl acetate, the three parameters were optimized using vapour pressure and saturated liquid density in the temperature range of 298.15 K to 0.9$T_c$, where $T_c$ is the critical temperature. The data for the vapour pressure, saturated liquid density, and critical temperature were obtained from DIPPR [51], and the objective function used for the propyl acetate is defined as

$$OF\left(m, \sigma, \frac{\varepsilon}{k_B}, \frac{\varepsilon^{AB}}{k_B}, k^{AB}\right) = \min \sum_{i=1}^{n} \left(\frac{P_i^{calc} - P_i^{DIPPR}}{P_i^{DIPPR}}\right)^2 + \left(\frac{\rho_i^{calc} - \rho_i^{exp\,2}}{\rho_i^{exp}}\right) \tag{31}$$

To compare our theoretical data with the experimental ones, we have used the average absolute percentage deviation calculated by using Eq. (28). The fitted parameters and *AAPD* are summarized in Table 11. From the deviations obtained, we observe that PC-SAFT represents the experimental density of pure fluids with very good accuracy (overall deviation = 0.44 %).

The modelling of the experimental density data in the temperature range (298.15 K to 323.15 K) was obtained with a fully predictive approach for the [BMIM][$BF_4$] + propyl acetate. The correct modelling of the interactions between cations or anions and propyl acetate molecules allowed for the correct modelling of the density of the binary mixtures at different temperatures. The deviation obtained was 0.44 %, and Fig. 9 shows the comparison of the model with the experimental data at different temperatures. From Fig. 9, a good qualitative and quantitative agreement with the experimental data is observed. Our model accurately captures the variation of the liquid density with the molar fraction of the ionic liquid and with temperature.

### 5.3. Theoretical evaluation of speed of sound

#### 5.3.1. Scaled Particle Theory

Scaled particle theory (SPT) [52,53] postulates that liquid molecules can be represented as rigid hard spheres, thereby circumventing the need to compute the radial distribution function that characterizes the equation of state for fluids. It integrates the intricacies of microscopic properties with the overarching principles of thermodynamic (macroscopic) properties [53]. In the theoretical estimation of $u$ values within binary mixtures [53], the SPT examines various geometrical configurations of the constituent molecules, including spherical, cubic, tetrahedral, disc A, disc B, disc C and disc D [54]. A number of researchers [55–57] utilized SPT to assess u values for binary mixtures. As per SPT, the equation of state for a fluid is articulated as

$$\frac{p}{\rho_N k_B T} = \frac{1 + \eta_H + \eta_H^2}{(1 - \eta_H)^3} \tag{32}$$

**Table 11**
Coefficients, $j_i$ of equation (26) for density, $\rho$/g·cm$^{-3}$, standard deviations, $\sigma$, $r^2$ and *AAPD* for [BMIM][$BF_4$] + propyl acetate mixtures at temperatures, $T$/K = (293.15 – 318.15).

| a)T/K | $j_0$ | $j_1$ | $j_2$ | $\sigma$ ($10^{-3}$) | $r^2$ | *AAPD* |
|---|---|---|---|---|---|---|
| 298.15 | 62.500 | -21.048 | 6.907 | 0.0141 | 1.000 | 0.0081 |
| 303.15 | 63.655 | -20.954 | 6.721 | 0.0132 | 1.000 | 0.0078 |
| 308.15 | 64.819 | -20.874 | 6.504 | 0.0126 | 1.000 | 0.0074 |
| 313.15 | 65.990 | -20.823 | 6.225 | 0.0135 | 1.000 | 0.0081 |
| 318.15 | 67.202 | -20.826 | 6.112 | 0.0128 | 1.000 | 0.0077 |
| 323.15 | 68.420 | -20.839 | 5.934 | 0.0137 | 1.000 | 0.0083 |

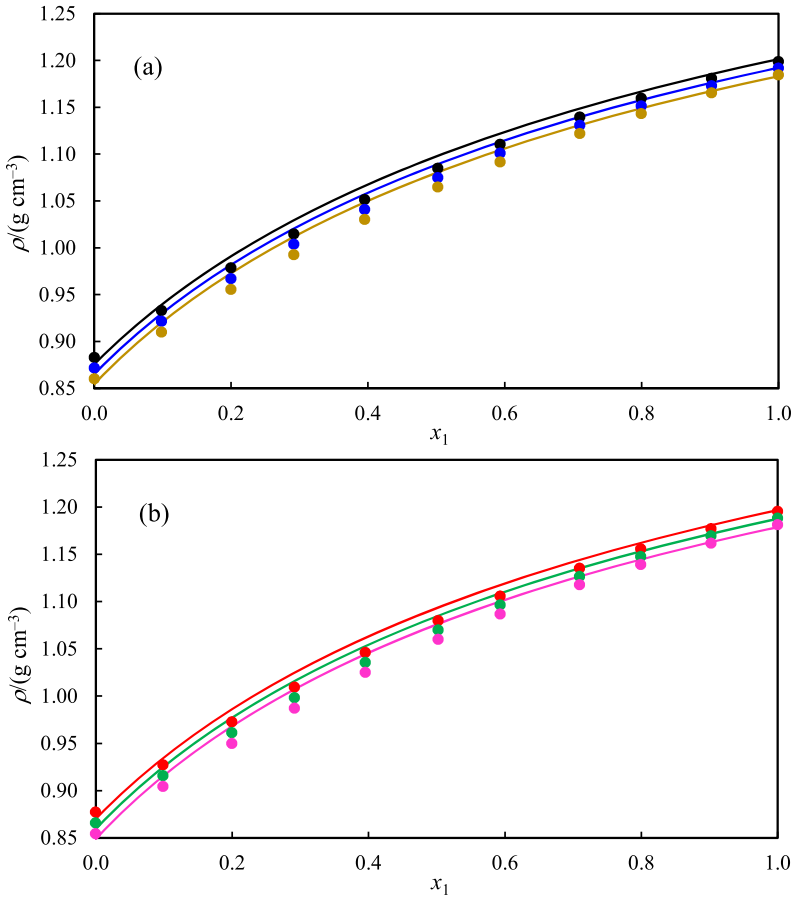


**Fig. 9.** Comparison between experimental density and calculated density using PC-SAFT EoS for the [BMIM][$BF_4$] + propyl acetate mixture at different temperatures and atmospheric pressure. Lines: theoretical results obtained with PC-SAFT and $k_{ij} = 0$. Circles: experimental data published in this manuscript, (a) black, 298.15 K; blue, 308.15 K; brown, 318.15 and (b) red, 303.15 K; green, 313.15 K; purple, 323.15 K.

In this context, $p$ denotes the pressure, while $\rho_N$ signifies the number density $N_A/V_o$, with $V_o$

Representing the ideal volume of the mixture. Additionally, $\eta_H = V_H\rho_N$, where $V_H$ refers to the hard-core volume of a molecule, $\eta_H$ indicates the hard-core volume per mole of molecules, and $k_B$ is the Boltzmann constant. In the context of a mixture comprising hard convex molecules, the equation of state is delineated [52,53]

$$\frac{p}{\rho_N k_B T} = \frac{1}{(1 - V\rho_N)} + \frac{AB\rho_N}{(1 - V\rho_N)^2} + \frac{B^2 C\rho_N^2}{3(1 - V\rho_N)^3} \tag{33}$$

$$A = \sum x_i \overline{R}_{i*} B = \sum x_i S_i, C = \sum x_i \overline{R}_i^2, V = \sum x_i V_H \tag{34}$$

where $\overline{R}_i$, $S_i$ and are the mean radius of curvature and surface area, respectively, of a molecule of species $i$. The values of $\overline{R}$, $S$ and $V_H$ for considered shapes are recorded in Table 12.

The pressure derivative is related to $u$ through the relation

**Table 12**
Coefficients, $j_i$ of equation (26) for speed of sound, $u$/m·s$^{-1}$, standard deviations, $\sigma$, $r^2$ and *AAPD* for [BMIM][$BF_4$] + propyl acetate mixtures at temperatures, $T$/K = (293.15 – 318.15).

| b) T/K | $j_0$ | $j_1$ | $j_2$ | $\sigma$ | $r^2$ | *AAPD* |
|---|---|---|---|---|---|---|
| 298.15 | 0.389 | 17.362 | -8.156 | 0.0078 | 1.000 | 0.0036 |
| 303.15 | -8.286 | 15.570 | -8.275 | 0.0040 | 1.000 | 0.0018 |
| 308.15 | -17.262 | 13.444 | -9.025 | 0.0169 | 1.000 | 0.0076 |
| 313.15 | -27.245 | 11.182 | -8.601 | 0.0032 | 1.000 | 0.0014 |
| 318.15 | -37.585 | 8.701 | -7.095 | 0.0201 | 1.000 | 0.0085 |
| 323.15 | -48.397 | 6.161 | -3.849 | 0.0195 | 1.000 | 0.0077 |

$$\gamma\left(\frac{dp}{d\rho}\right)_T = u^2 \tag{35}$$

where $\rho$ is molecular density and $\gamma$ is the ratio of specific heats. Equations (33) and (35), gives

$$\frac{Mu^2}{\gamma RT} = \frac{1}{(1 - V\rho_N)^2} + \frac{2AB\rho_N}{(1 - V\rho_N)^3} + \frac{B^2 C\rho_N^2}{(1 - V\rho_N)^4} \tag{36}$$

Equation (36) is used to theoretically evaluate $u$ values for the binary mixtures. For pure liquids, equation (36) can be improved by including the dimensionless shape parameters, $X = \overline{R}S/V_H$ and $\eta_H = V_H\rho_N$ as

$$\frac{Mu^2}{\gamma RT} = \frac{[1 + (X - 1)\eta_H]^2}{(1 - \eta_H)^4} \tag{37}$$

Its solution is attained as [54]

$$\eta_H = K - \sqrt{K^2 + L - 1} \tag{38}$$

where $K = 1 + L(X-1)/2$ and $L = \sqrt{\gamma RT/Mu^2}$. The $\overline{R}$ and $S$ for a molecule can be written as $\overline{R} = YV_H^{1/3}$ and $S = Z\overline{R}^2$, where the parameters $Y$ and $Z$ are associated with the shape of molecules. The values of $X$, $Y$ and $Z$ were evaluated for several assumed shapes and are given in Table 13. The values of $\eta_H$ are given in Table 14.

The theoretical $u$ for [BMIM][$BF_4$] + propyl acetate mixtures was derived from SPT for 49 configurations of designated shapes to the component molecules. The optimal configuration of shapes for participating molecules, exhibiting the minimal discrepancy between

**Table 13**
Parameters of the fluids required in PC-SAFT EoS and the deviations in the compressed liquid density with respect to the experimental values for pure components.

| Fluid | $m$ | $\sigma$/Å | $\varepsilon/k_B$/K | $\kappa^{AB}$ | $\varepsilon^{AB}/k_B$/K | $\%AAPD(\rho)$ |
|---|---|---|---|---|---|---|
| [BMIM][$BF_4$] | 10.43241 | 2.99966 | 298.76 | 0.31774 | 5620.43 | 0.12 |
| Propyl acetate | 3.81176 | 3.40862 | 234.95 | - | - | 0.75 |
| Overall | | | | | | 0.44 |

**Table 14**
Molecular parameters for various shapes.

| Shape | Size | $\overline{R}$ | $S$ | $V_H$ |
|---|---|---|---|---|
| Sphere | Radius=$a$ | $A$ | $4\pi a^2$ | $4\pi a^3/3$ |
| Cube | Side=$l$ | $3l/4$ | $6l^2$ | $l^3$ |
| Tetrahedron | Side=$l$ | $3larctan\sqrt{2}/2\pi$ | $\sqrt{3}l^2$ | $(\sqrt{2}/12)l^3$ |
| Discs | Radius = $a$ and Depth = $l$ | | | |
| Disc A | $l = a$ | $(\pi + 1)a/4$ | $4\pi a^2$ | $\pi a^3$ |
| Disc B | $l = a/4$ | $(\pi + 0.25)a/4$ | $5\pi a^2/2$ | $\pi a^3/4$ |
| Disc C | $l = a/2$ | $(\pi + 0.50)a/4$ | $3\pi a^2$ | $\pi a^3/2$ |
| Disc D | $l = a/10$ | $(\pi + 0.10)a/4$ | $11\pi a^2/5$ | $\pi a^3/10$ |

experimental and theoretical u values, was ascertained through the application of *AAPD* derived from equation (28). The experimental and theoretically calculated $u$ values for these mixtures, which have the most appropriate combination of molecular shapes, at 298.15, 308.15 and 318.15 K are presented in Table 15, Table 17.

A meticulous of examination of Table 15 reveals that the shapes of IL and propyl acetate molecules are influenced by variations in temperature. The deviation between experimental and theoretically calculated $u$ is 0.233 % for IL + propyl acetate mixtures when IL is assigned disk C shape and propyl acetate molecules are assigned tetrahedron shape at 298.15 K, deviation is 0.096 % when IL is assigned spherical shape and propyl acetate molecules assigned tetrahedron shape at 308.15 K, and the deviation is 0.094 % when IL is assigned disk A shape and propyl acetate molecules assigned disc D shape at 318.15 K. The deviation is lowest at 318.15 K. The SPT predicted the $u$ for these mixtures reasonably well.

### 5.3.2. Collision factor theory

The $u$ for mixtures can be calculated using Schaff's collision factor theory (CFT) [58], which is given by following relation for $u$ of pure liquids

$$u = u_\infty S r_j = u_\infty SB/V_m \tag{39}$$

where $u_\infty = 1600$ m $s^{-1}$, $S$ is the collision factor and $r_j = B/V_m$ is the space filling factor and $B$ is the actual volume of the molecule per mole, given by

$$B = \frac{4}{3}\pi r_m N_A \tag{40}$$

where $r_m$ is the molecular radius and $N_A$ is the Avogadro number. The $r_m$ has been calculated using the relation [59]

**Table 15**
Shape parameters.

| Shape | $X = \overline{R}S/V_H$ | $Y = \overline{R}/\sqrt[3]{V_H}$ | $Z = S/\overline{R}^2$ |
|---|---|---|---|
| Sphere | 3.0000 | 0.6204 | 12.5664 |
| Cube | 4.5000 | 0.7500 | 10.6666 |
| Tetrahedron | 6.7035 | 0.9303 | 8.3247 |
| Disc A | 4.1416 | 0.7070 | 11.7218 |
| Disc B | 8.4790 | 0.9190 | 10.9244 |
| Disc C | 5.4624 | 0.7832 | 11.3712 |
| Disc D | 17.8274 | 1.1920 | 10.5253 |

$$r_m = \alpha\left[1 - \beta\left\{\left(1 + \frac{1}{\beta}\right)^{1/2} - 1\right\}\right]^{1/3} \tag{41}$$

where $\alpha = (3V/16\pi N_A)^{1/3}$ and $\beta = (\gamma RT/Mu^2)$, $\gamma$ is the ratio of molar specific heats and $R$ is universal gas constant. The application of this concept to binary liquid mixtures was undertaken by Nutsch-Kuhnkies [60] for the calculation of $u_{CFT}$ for these mixtures

$$u_{CFT} = u_\infty[x_1S_1 + (1-x_1)S_2][x_1B_1 + (1-x_1)B_2]/V_m \tag{42}$$

### 5.3.3. Nomoto relation

The relationship established by Nomoto (NOM) can be employed to theoretically evaluate the $u$ for binary mixtures based on the data pure components utilising the specified relation [61]

$$u_{NOM} = \left[\left(x_1R_{m,1} + (1-x_1)R_{m,2}\right)/\left(x_1V_{m,1} + (1-x_1)V_{m,2}\right)\right]^3 \tag{43}$$

where $R_m = V_m u^{1/3}$ is the molar sound velocity.

### 5.3.4. van Dael and Vangeel ideal mixing relation

Using the pure component data, the $u$ in liquid mixes can be theoretically evaluated using the van Dael and Vangeel (VDV) ideal mixing relation [62], Table 18.

$$u_{VDV} = \left[\frac{1}{(x_1M_1 + (1-x_1)M_2)}\right]^{1/2}\left[\frac{x_1}{(M_1u_1^2)} + \frac{1-x_1}{(M_2u_2^2)}\right]^{-1/2} \tag{44}$$

### 5.3.5. Junjie relation

Using pure component data and the Junjie relation [63]. It is also possible to theoretically Fig. out the $u$ in liquid mixtures.

$$u_{Junjie} = \frac{x_1V_{m,1} + (1-x_1)V_{m,2}}{(x_1M_1 + (1-x_1)M_2)^{1/2}}\left[\frac{x_1V_{m,1}^2}{M_1u_1^2} + \frac{(1-x_1)V_{m,2}^2}{M_2u_2^2}\right]^{-1/2} \tag{45}$$

Table 16 shows the experimentally and theoretically estimated values of the speed of sound, $u_{SPT}$, $u_{CFT}$, $u_{NOM}$, $u_{VDV}$ and $u_{Junjie}$ from several models, as well as AAPD evaluated by the equation (28) at 298.15 K. A thorough look at Table 16 shows that all the theories and relationships

**Table 16**
Values of the hard-core volume of molecules per mole, $\eta_H$ for various shapes for [BMIM][$BF_4$] and propyl acetate at temperatures, $T$/K = (298.15, 308.15 and 318.15) calculated from equation (38).

| Shape | 298.15 K | 308.15 K | 318.15 K |
|---|---|---|---|
| [BMIM][$BF_4$] | | | |
| Sphere | 0.9220 | 0.9208 | 0.9196 |
| Cube | 0.9055 | 0.9041 | 0.9026 |
| Tetrahedron | 0.8862 | 0.8844 | 0.8827 |
| Disc A | 0.9091 | 0.9077 | 0.9064 |
| Disc B | 0.8730 | 0.8711 | 0.8693 |
| Disc C | 0.8965 | 0.8950 | 0.8934 |
| Disc D | 0.8218 | 0.8193 | 0.8167 |
| Propyl acetate | | | |
| Sphere | 0.8904 | 0.8875 | 0.8846 |
| Cube | 0.8679 | 0.8645 | 0.8610 |
| Tetrahedron | 0.8417 | 0.8377 | 0.8336 |
| Disc A | 0.8728 | 0.8696 | 0.8662 |
| Disc B | 0.8241 | 0.8197 | 0.8152 |
| Disc C | 0.8557 | 0.8521 | 0.8483 |
| Disc D | 0.7564 | 0.7507 | 0.7448 |

**Table 17**
Experimental and SPT calculated speeds of sound, $u_{Expt}$ and $u_{SPT}$ for suitable assigned shapes along with *AAPD* for [BMIM][$BF_4$] + propyl acetate mixtures at temperature, $T$/K = 298.15, 308.15 and 318.15.

| $x_1$ | 298.15 K | | 308.15 K | | 318.15 K | |
|---|---|---|---|---|---|---|
| | $u_{Expt}$ | $u_{SPT}$ | $u_{Expt}$ | $u_{SPT}$ | $u_{Expt}$ | $u_{SPT}$ |
| | Disc C + tetrahedron | | Spherical + tetrahedron | | Disc A + disc D | |
| 0.0000 | 1165.1 | 1165.1 | 1122.6 | 1122.6 | 1080.1 | 1080.1 |
| 0.0985 | 1192.7 | 1197.8 | 1146.6 | 1149.3 | 1101.8 | 1103.8 |
| 0.1999 | 1227.3 | 1234.5 | 1178.6 | 1181.4 | 1130.0 | 1132.5 |
| 0.2916 | 1262.6 | 1269.5 | 1211.4 | 1213.8 | 1160.3 | 1162.4 |
| 0.3955 | 1305.5 | 1310.5 | 1252.5 | 1253.6 | 1199.4 | 1200.4 |
| 0.5022 | 1351.6 | 1353.9 | 1297.9 | 1297.7 | 1244.3 | 1244.0 |
| 0.5932 | 1391.8 | 1391.7 | 1338.8 | 1337.8 | 1286.0 | 1285.0 |
| 0.7095 | 1442.5 | 1440.7 | 1393.3 | 1391.9 | 1344.0 | 1342.8 |
| 0.7994 | 1481.2 | 1479.0 | 1437.0 | 1436.0 | 1392.8 | 1392.0 |
| 0.9023 | 1524.6 | 1523.2 | 1489.0 | 1488.9 | 1454.5 | 1453.7 |
| 1.0000 | 1564.9 | 1564.9 | 1541.2 | 1541.2 | 1518.0 | 1518.0 |
| *AAPD* = | | 0.233 | | 0.096 | | 0.094 |

**Table 18**
Theoretically calculated speeds of sound, $u_{SPT}$, $u_{CFT}$, $u_{NOM}$, $u_{VDV}$ and $u_{Junjie}$ using various theories along with average absolute percentage deviation, *AAPD* and experimentally measured speed of sound, $u_{Expt}$ for [BMIM][$BF_4$] + propyl acetate mixtures at temperature, $T$/K = 298.15.

| $x_1$ | $u_{Expt}$ | $u_{SPT}$ | $u_{CFT}$ | $u_{NOM}$ | $u_{VDV}$ | $u_{Junjie}$ |
|---|---|---|---|---|---|---|
| 0.0000 | 1165.1 | 1165.1 | 1165.1 | 1165.1 | 1165.1 | 1165.1 |
| 0.0985 | 1192.7 | 1197.8 | 1207.7 | 1220.6 | 1144.2 | 1189.3 |
| 0.1999 | 1227.3 | 1234.5 | 1250.3 | 1272.7 | 1133.6 | 1218.3 |
| 0.2916 | 1262.6 | 1269.5 | 1288.1 | 1316.2 | 1132.8 | 1247.7 |
| 0.3955 | 1305.5 | 1310.5 | 1330.2 | 1361.6 | 1141.9 | 1284.3 |
| 0.5022 | 1351.6 | 1353.9 | 1372.8 | 1404.4 | 1163.1 | 1325.4 |
| 0.5932 | 1391.8 | 1391.7 | 1408.6 | 1438.3 | 1192.2 | 1363.2 |
| 0.7095 | 1442.5 | 1440.7 | 1453.9 | 1478.3 | 1248.3 | 1415.2 |
| 0.7994 | 1481.2 | 1479.0 | 1488.5 | 1506.9 | 1311.2 | 1458.3 |
| 0.9023 | 1524.6 | 1523.2 | 1527.8 | 1537.7 | 1415.0 | 1511.1 |
| 1.0000 | 1564.9 | 1564.9 | 1564.9 | 1564.9 | 1564.9 | 1564.9 |
| *AAPD* = | | 0.233 | 0.871 | 2.070 | 7.302 | 0.933 |

used to forecast the $u$ data are rather accurate, with AAPDs ranging from 0.233 % to 2.07 %. The van Dael and Vangeel relationship, on the other hand, had the greatest difference, 7.302 %. SPT did the best job of predicting the $u$ data for all these binary mixtures, with the lowest AAPDs being 0.233 %. This is because this theory examines the most compatible morphologies of the molecules in the combination to determine $u$ values.

## 6. Analysis of FT-IR spectra

In addition to the physicochemical study, the nature and degree of intermolecular interactions between ILs with organic solvents can be qualitatively analysed using FT-IR spectra. To achieve this objective, the FT-IR spectra of pure [BMIM][$BF_4$], propyl acetate and their near-equimolar mixture have been utilised to investigate interactions between [BMIM][$BF_4$] and propyl acetate at the atomic level.

Fig. 10 shows the spectra for pure compounds and their binary solution at the same molar concentration. The FT-IR spectra of propyl acetate show a sharp band for the carbonyl C=O stretch at 1738.94 $cm^{-1}$, with C–H stretching vibrations occurring between 2995.97 and 2911.2 $cm^{-1}$. It is known that less extensive H-bonding produces a sharp peak at higher frequencies, while more extensive bonding results in a larger peak at lower frequencies [64].

A sharp peak is observed for pure propyl acetate at 1738.94 $cm^{-1}$ confirms absence of H-bonding. But on addition of [BMIM][$BF_4$] to propyl acetate, the FT-IR intensities for equimolar mixture, exhibited significant changes in frequency of peaks; which may be attributed to the breaking/formation of intermolecular interactions (mainly H-bonding and ion-dipole interactions) at equimolar concentration. On addition of [BMIM][$BF_4$] to propyl acetate a red shift (of 12.63 $cm^{-1}$) in C=O stretch is observed in propyl acetate, from 1738.94 to 1726.29 $cm^{-1}$, clearly indicating the formation of intermolecular hydrogen bond between [BMIM][$BF_4$] and carbonyl oxygen of propyl acetate.

The two bands manifest within the spectral range of 3100 to 3200 $cm^{-1}$, attributed to C-H stretching vibrations in the imidazolium ring, specifically at 3116.0 $cm^{-1}$ and 3161.28 $cm^{-1}$ in pure [BMIM][$BF_4$]. The presence of these two C-H stretching peaks suggests the existence of an imidazolium ring in two distinct environments, such as dissociated ions and ion pairs [65]. Upon the introduction of propyl acetate, discernible alterations were observed, indicating that the peaks corresponding to C-H stretching bands exhibit a shift to marginally lower frequencies. The transition can be attributed to the interaction of ion-dipole forces and hydrogen bonding between the Nitrogen atoms of the aromatic imidazolium cation in [BMIM][$BF_4$] and the carbonyl group of propyl acetate.

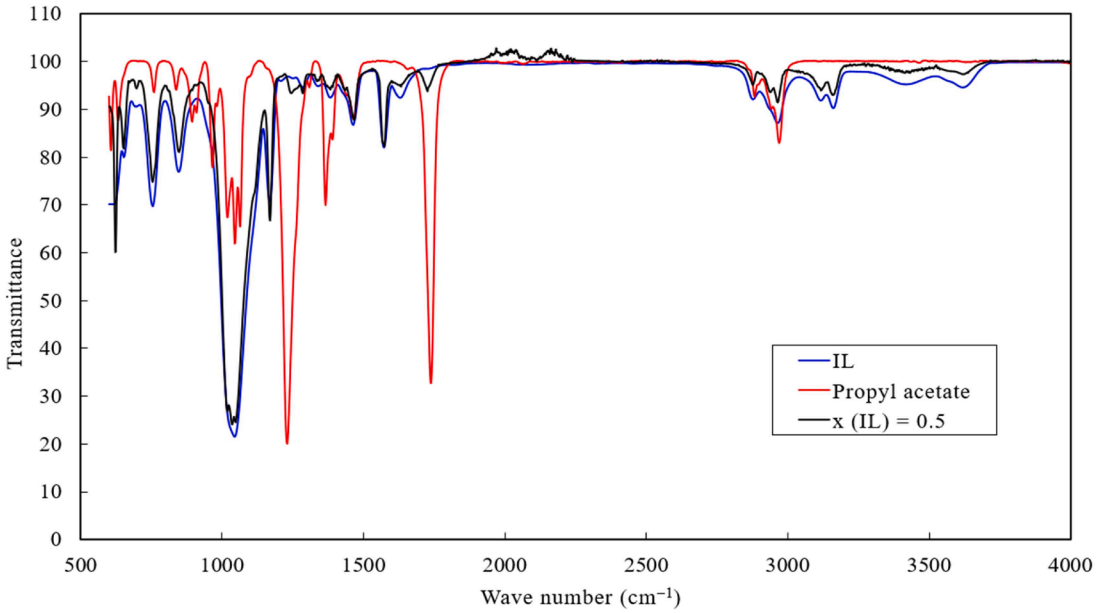


**Fig. 10.** FTIR spectra of pure [BMIM][$BF_4$], blue line; pure propyl acetate, red line and equimolar ($x_{IL}$ = 0.5) mixture of [BMIM][$BF_4$] + ethyl acetate, black line.

The FT-IR distinctly indicates that the incorporation of [BMIM][$BF_4$] into polar propyl acetate markedly affects (a) the C-H vibration of the [BMIM] cation, (b) the C=O stretch of propyl acetate, and (c) the C-O stretch of Propyl acetate. Consequently, the positioning and intensities of peaks in the IR data concerning the hydrogen bonding and ion-dipole interactions between [BMIM][BF] and propyl acetate molecules provide robust support for the conclusions derived from the excess properties. Earlier investigations have yielded analogous conclusions regarding the binary systems of [BMIM][$PF_6$] and [BMIM][$BF_4$] combined with N-Vinyl-2-Pyrrolidinone [66,67], [BMIM][$PF_6$] with alkyl acetates [21], and [BMIM][$PF_6$] with 2-pyrrolidinone [68].

## 7. Conclusion

The densities, $\rho$ and speeds of sound, $u$ were measured for the binary mixtures of [BMIM][$BF_4$] with propyl acetate at the temperatures 298.15, 303.15, 308.15, 313.15, 318.15 and 323.15 K throughout the mole fraction range at atmospheric pressure. Using the measured data, $V_m^E$, $\kappa_s^E$, $K_{s,m}^E$, $u^E$ and $\alpha_p^E$ have been calculated. The $\overline{V}_{m,1}$, $\overline{V}_{m,2}$, $\overline{K}_{s,m,1}$, $\overline{K}_{s,m,2}$, $\overline{V}_{m,1}^E$, $\overline{V}_{m,2}^E$, $\overline{K}_{s,m,1}^E$, $\overline{K}_{s,m,2}^E$, $\overline{V}_{m,1}^*$, $\overline{V}_{m,2}^*$, $\overline{V}_{m,1}^{*E}$, $\overline{V}_{m,2}^{*E}$, $\overline{K}_{s,m,1}^*$, $\overline{K}_{s,m,2}^*$, $\overline{K}_{s,m,1}^{*E}$ and $\overline{K}_{s,m,2}^{*E}$ of the components have also been calculated. The PFP model shows close agreement between experimental and theoretical $V_m^E$ values, demonstrating its reliability in describing the volumetric behaviour of these mixtures. The Jouyban-Acree model demonstrated how composition and temperature affect the $\rho$ and $u$ values of various mixtures. In this study, we also used PC-SAFT for the modelling of $\rho$ data of these mixtures. The use of A 2B scheme with a positive and a negative site for ionic liquid and a scheme with two negative sites for propyl acetate, successfully allowed to correctly model the experimental density with the mole fraction as well as with temperature. Among various theories and models utilized to calculate $u$ values of these mixtures theoretically, SPT predicted the data best. The results indicated the presence of ion-dipole and H-bonding interactions among [BMIM][$BF_4$] and propyl acetate molecules in these mixtures, which are well reinforced by FTIR spectra also.

## CRediT authorship contribution statement

**M. Durga Bhavani:** Writing – original draft, Methodology, Investigation, Data curation. **T.S. Krishna:** Writing – original draft, Supervision, Methodology, Conceptualization. **A. Hernandez:** Writing – original draft, Software, Formal analysis, Conceptualization. **A.K. Nain:** Writing – review & editing, Supervision, Methodology, Conceptualization.

## Declaration of competing interest

The authors declare that they have no known competing financial interests or personal relationships that could have appeared to influence the work reported in this paper.

The author (A.K. Nain) is an Editorial Board Member/Editor-in-Chief/Associate Editor/Guest Editor for *[Journal of Chemical Thermodynamics]* and was not involved in the editorial review or the decision to publish this article.

## Data availability

The authors are unable or have chosen not to specify which data has been used.

## References


[1] J.D. Holbrey, K.R. Seddon, Clean Prod. Proc 1 (1999) 223–236.
[2] T. Welton, Chem. Rev. 99 (1999) 2071–2083.
[3] T.M. Letcher, N. Deenadayalu, J. Chem. Thermodyn. 35 (2003) 67–76.
[4] J.G. Huddleston, H.D. Willauer, R.P. Swatloski, A.E. Visser, R.D. Rogers, Chem. Commun. (1998) 1765–1766.
[5] J. Dupont, R.F. de Souza, P.A.Z. Suarez, Chem. Rev. 102 (2002) 3667–3692.
[6] H. Olivier-Bourbigou, L. Magna, J. Mol. Catal. A Chem. 182 (2002) 419–437.
[7] B.C. Ranu, S.S. Dey, A. Hajra, Tetrahedron 59 (2003) 2417–2421.
[8] J.N. Barisci, G.G. Wallace, D.R. MacFarlane, R.H. Baughman, Electrochem. Commun. 6 (2004) 22–27.
[9] Z. Li, H. Liu, Y. Liu, P. He, J. Li, J. Phys. Chem. B. 108 (2004) 17512–17518.
[10] L.P.N. Rebelo, J.N.C. Lopes, J.M.S.S. Esperanc, E. Filipe, J. Phys. Chem. B. 109 (2005) 6040–6043.
[11] J.G. Huddleston, A.E. Visser, W.M. Reichert, H.D. Willauer, G.A. Broker, R. D. Rogers, Green Chem 3 (2001) 156–164.
[12] T. Nishida, Y. Tashiro, M. Yamamoto, J. Fluorine Chem. 120 (2003) 135–141.
[13] M. Koel, Proc. Estonian Acad. Sci. Chem. 49 (2000) 145–155.
[14] A. Jouyban, J. Soleymani, F. Jafari, M. Khoubnasabjafari, W.E. Acree Jr., J. Chem. Eng. Data 58 (2013) 1523–1528.
[15] A. Jouyban, W.E. Acree Jr., J. Mol. Liq. 323 (2021) 115054.
[16] J. Gross, G. Sadowski, Ind. Eng. Chem. Res. 40 (4) (2001) 1244–1260.
[17] J. Gross, G. Sadowski, Ind. Eng. Chem. Res. 41 (22) (2002) 5510–5515.
[18] P. Yella Reddy, T.S. Krishna, M. Gowrisankar, K. Siva Kumar, Ch.N.S.S. Pavan Kumar, J. Chem. Thermodyn. 154 (2021) 106316.
[19] E. Scholz, Karl Fischer Titration, Springer-Verlag, Berlin, 1984.
[20] T.S. Krishna, P.V.V.S. Rama Rao, K. Narendra, D.B.K. Kumar, D. Ramachandran, J. Mol. Liq. 339 (2021) 117187.
[21] A.K.Nain Nidhi, J. Chem. Thermodyn. 198 (2024) 107339.
[22] G. Douheret, M.I. Davis, J.C.R. Reis, M.J. Blandamer, Chem. Phys. Chem. 2 (2001) 148–161.
[23] G. Douheret, M.I. Davis, J.C.R. Reis, I.J. Fjellanger, M.B. Vaage, H. Hoiland, Phys. Chem. Chem. Phys. 4 (2002) 6034–6042.
[24] G.C. Benson, O. Kiyohara, J. Chem. Thermodyn. 11 (1979) 1061–1064.
[25] C.A. Cerdeirina, C.A. Tovar, D.G. Lez-Salgado, E. Carballo, L. Romano, Phys. Chem. Chem. Phys. 3 (2001) 5230–5236.
[26] R.C. Reid, J.M. Prausnitz, B.E. Poling, The Properties of Gases and Liquids, 4th Edn., McGraw Hill Inc., New York, 1987, p. 139.
[27] O. Redlich, A.T. Kister, Ind. Eng. Chem. 40 (1948) 345. –34.
[28] L. Crowhurst, P.R. Mawdsley, J.M. Perez-Arlandis, P.A. Salter, T. Welton, Phys. Chem. Chem. Phys. 5 (2003) 2790.
[29] P.V.V.S. Rama Rao, T.S. Krishna, D. Ramachandran, J. Chem. Thermodyn. 141 (2020) 105906.
[30] P.V.S.S Rama Rao, T.S. Krishna, R. Dey, D. Ramachandran, J. Chem. Thermodyn. 156 (2021) 106383.
[31] B. Kumar, T. Singh, K. Srinivasa Rao, A. Pal, A. Kumar, J. Chem. Thermodyn. 44 (2012) 121–127.
[32] R. Hayes, G.G. Warr, R. Atkin, Chem. Rev. 115 (2015) 6357–6426.
[33] G.V.A.R. Rao, V. Sarma, C. Rambabu, Indian J. Chem. A 43 (2004) 2518–2528.
[34] R. Sadeghi, H. Shekaari, R. Hosseini, Int. J. Thermophys. 30 (2009) 1491–1509.
[35] F. Kawaizumi, M. Ohno, Y. Miyahara, Bull. Chem. Soc. Jpn. 50 (1977) 2229–2233.
[36] O. Prakash, S. Sinha, Acustica 54 (1984) 223–225.
[37] M.M. Alavianmehr, N. Hemmati, H. Ghodrati, Phy. Chem. Liq. 55 (2017) 85–99.
[38] H. Wang, W. Liu, J. Huang, J. Chem. Thermodyn. 36 (2004) 743–752.
[39] B. Hawrylak, K. Gracie, R. Palepu, J. Solut. Chem. 27 (1998) 17–31.
[40] H. Iloukhani, R. Ghorbani, J. Solut. Chem. 27 (1998) 141–149.
[41] T.M. Aminabhavi, V.B. Patil, K. Banerjee, R.H. Balundgi, Bull. Chem. Soc. Jpn. 72 (1999) 1187–1195.
[42] S.K. Mehta, R.K. Chauhan, J. Solut. Chem. 26 (1997) 295–308.
[43] L. Hall, Phys. Rev. 73 (1948) 775–784.
[44] A. Cipiciani, G. Onori, G. Savelli, Chem. Phys. Lett. 143 (1988) 505–509.
[45] P. Suneetha, T.S. Krishna, M. Gowrisankar, K. Ravindhranath, D. Ramchandran, J. Chem. Thermodyn. 108 (2017) 181–192.
[46] E.I. Cooper, E.J. O'Sullivan, Proc. Electrochem. Soc. 16 (1992) 386–396.
[47] E. Vercher, P.J. Miguel, F.J. Llopis, A.V. Orchillés, A. Martínez-Andreu, J. Chem. Eng. Data 57 (2012) 1953–1963.
[48] A. Pal, B. Kumar, T.S. Kang, Fluid Phase Equilib 358 (2013) 241–249.
[49] F. Shaahmadi, B.H. Shahraki, A. Farhadi, J. Chem. Thermodyn. 141 (2020) 105922.
[50] M.R. Curras, J. Vijande, M.M. Pineiro, L. Lugo, J. Salgado, J. Garcia, Ind. Eng. Chem. Res. 50 (2011) 4065–4076.
[51] T.E. Daubert, R.P. Danner, Taylor & Francis: Bristol, PA, 2004.
[52] H. Reiss, H.L. Frisch, J.L. Lebowitz, J. Chem. Phys. 31 (1959) 369–380.
[53] H. Reiss, H.L. Frisch, E. Helfand, J.L. Lebowitz, J. Chem. Phys. 32 (1960) 119–125.
[54] D.M.T. Smith, H. Reiss, J. Chem. Phys. 53 (1970) 4015–4026.
[55] R.M. Gibbons, Mol. Phy. 17 (1969) 81–86.
[56] K. Rajagopal, S. Chenthilnath, Chin. J. Chem. Eng. 18 (2010) 804–816.
[57] K. Rajagopal, S. Chenthilnath, Thermochim. Acta 498 (2010) 45–53.
[58] W. Schaaffs, Acta Acust. United Acust. 33 (1975) 272–276.
[59] R.V.G. Rao, V. Venkatseshaiah, Z. Phys. Chem. 242 (1969) 193–199.
[60] R. Nutsch-Kunkies, Acustica 15 (1965) 383–385.
[61] O. Nomoto, J. Phys. Soc. Jpn. 13 (1958) 1528–1532.
[62] W. van Dael, E. Vangeel, in: Proc. Int. Conf. on Calorimetric and Thermodynamics, Warsaw, 1955, p. 555.
[63] Z. Junjie, J. Chin. Univ. Sci. Techn. 14 (1984) 298–300.
[64] P.K. Pandey, A. Awasthi, A. Awasthi, Chem. Phys. 423 (2013) 119–126.
[65] A. Pal, B. Kumar, J. Mol. Liq. 163 (2011) 128–134.

[66] B. Goddu, M.M. Tadavarthi, V.K. Tadekoru, J.N. Guntupalli, J. Chem. Eng. Data 64 (2019) 2303–2319.
[67] G.R. Sunkara, M.M Tadavarthi, V.K. Tadekoru, S.K. Tadikonda, S.R. Bezawada, J. Chem. Eng. Data 60 (2015) 886–894.
[68] V.S. Rao, M.S. Reddy, K.T.S.S. Raju, B.L. Rani, H. Babu, J. Solut. Chem. 47 (2018) 430–448.